



HAL
open science

Recursive marginal quantization of an Euler scheme with applications to local volatility models

Abass Sagna, Gilles Pagès

► **To cite this version:**

Abass Sagna, Gilles Pagès. Recursive marginal quantization of an Euler scheme with applications to local volatility models. 2014. hal-00809313v2

HAL Id: hal-00809313

<https://hal.science/hal-00809313v2>

Preprint submitted on 11 Jul 2014 (v2), last revised 20 Apr 2015 (v3)

HAL is a multi-disciplinary open access archive for the deposit and dissemination of scientific research documents, whether they are published or not. The documents may come from teaching and research institutions in France or abroad, or from public or private research centers.

L'archive ouverte pluridisciplinaire **HAL**, est destinée au dépôt et à la diffusion de documents scientifiques de niveau recherche, publiés ou non, émanant des établissements d'enseignement et de recherche français ou étrangers, des laboratoires publics ou privés.

Recursive marginal quantization of an Euler scheme with applications to local volatility models

GILLES PAGÈS * ABASS SAGNA † ‡

Abstract

We propose a new approach to quantize the marginals of the discrete Euler diffusion process. The method is built recursively and involves the conditional distribution of the marginals of the discrete Euler process. Analytically, the method raises several questions like the analysis of the induced quadratic quantization error between the marginals of the Euler process and the proposed quantizations. We show in particular that at every discretization step t_k of the Euler scheme, this error is bounded by the cumulative quantization errors induced by the Euler operator, from times $t_0 = 0$ to time t_k . For numerics, we restrict our analysis to the one dimensional setting and show how to compute the optimal grids using a Newton-Raphson algorithm. We then propose a close formula for the companion weights and the transition probabilities associated to the proposed quantizations. This allows us to quantize in particular diffusion processes in local volatility models by reducing dramatically the computational complexity of the search of optimal quantizers while increasing their computational precision with respect to the algorithms commonly proposed in this framework. Numerical tests are carried out for the Brownian motion and for the pricing of European options in a local volatility model. A comparison with the Monte Carlo simulations shows that the proposed method is more efficient (w.r.t. both computational precision and time complexity) than the Monte Carlo method.

1 Introduction

Optimal quantization method appears first in [23] where the author studies in particular the optimal quantization problem for the uniform distribution. It has become an important field of information theory since the early 1940's. A common use of quantization is the conversion of a continuous signal into a discrete signal that assumes only a finite number of values.

Since then, optimal quantization is applied in many fields like in Signal Processing, in Data Analysis, in Computer Sciences and recently in Numerical Probability from the seminal work [13]. Its application to Numerical Probability relies on the possibility to discretize a random vector X taking infinitely many values by a discrete random vector \hat{X} valued in a set of finite cardinality. This allows to approximate either expectations of the form $\mathbb{E}f(X)$ or more significantly some conditional expectations like $\mathbb{E}(f(X)|Y)$ (by quantizing both random variables X and Y). Optimal quantization is used to solve some problems emerging in Quantitative Finance as optimal stopping problems (see [1, 2]),

*Laboratoire de Probabilités et Modèles aléatoires (LPMA), UPMC-Sorbonne Université, UMR CNRS 7599, case 188, 4, pl. Jussieu, F-75252 Paris Cedex 5, France. E-mail: gilles.pages@upmc.fr

†ENSIIE & Laboratoire de Mathématiques et Modélisation d'Evry (LaMME), Université d'Evry Val-d'Essonne, UMR CNRS 8071, 23 Boulevard de France, 91037 Evry. E-mail: abass.sagna@ensiie.fr.

‡The first author benefited from the support of the Chaire "Risques financiers", a joint initiative of École Polytechnique, ENPC-ParisTech and UPMC, under the aegis of the Fondation du Risque. The second author benefited from the support of the Chaire "Markets in Transition", under the aegis of Louis Bachelier Laboratory, a joint initiative of École polytechnique, Université d'Évry Val d'Essonne and Fédération Bancaire Française.

the pricing of swing options (see [4]), stochastic control problems (see [7, 15]), nonlinear filtering problems (see e.g. [14, 20, 6, 21]), the pricing of barrier options (see [22]).

In Quantitative Finance, several problems of interest amounts to the estimation of quantities of the form (for a given Borel function $f : \mathbb{R}^d \rightarrow \mathbb{R}$)

$$\mathbb{E}[f(X_T)], \quad T > 0, \quad (1)$$

or involving terms like

$$\mathbb{E}[f(X_t)|X_s = x], \quad 0 < s < t, \quad (2)$$

related to a stochastic diffusion process $(X_t)_{t \in [0, T]}$ solution to the stochastic differential equation

$$dX_t = b(t, X_t)dt + \sigma(t, X_t)dW_t, \quad X_0 = x_0 \in \mathbb{R}^d, \quad (3)$$

where W is a standard q -dimensional Brownian motion starting at 0 and where the functions $b : [0, T] \times \mathbb{R}^d \rightarrow \mathbb{R}^d$ and the matrix-valued diffusion coefficient function $\sigma : [0, T] \times \mathbb{R}^d \rightarrow \mathbb{R}^{d \times q}$ are Borel measurable and satisfy some appropriate conditions which ensure the existence of a strong solution of the stochastic differential equation. Since in general the solution of (3) is not explicit we have first to approximate the continuous paths of the process $(X_t)_{t \in [0, T]}$ by a discretization scheme, typically, the Euler scheme. Given the (regular) time discretization mesh $t_k = k\Delta$, $k = 0, \dots, n$, $\Delta = T/n$, the "discrete time Euler process" $(\bar{X}_{t_k})_k$, $k = 0, \dots, n$, associated to the previous diffusion process $(X_t)_{t \in [0, T]}$ is recursively defined by

$$\bar{X}_{t_{k+1}} = \bar{X}_{t_k} + b(t_k, \bar{X}_{t_k})\Delta + \sigma(t_k, \bar{X}_{t_k})(W_{t_{k+1}} - W_{t_k}), \quad \bar{X}_0 = X_0.$$

Then, once we have access to the discretization scheme of the stochastic process $(X_t)_{t \in [0, T]}$, the quantities (1) and (2) can be estimated by

$$\mathbb{E}[f(\bar{X}_T)] \quad (4)$$

and

$$\mathbb{E}[f(\bar{X}_{t_{k+1}})|\bar{X}_{t_k} = x], \quad \text{when } t = t_{k+1} \text{ and } s = t_k. \quad (5)$$

Remark 1.1. (a) For smooth functions f or under hypoellipticity assumptions on σ (see e.g. [3, 24]), the estimation of $\mathbb{E}(f(X_T))$ by $\mathbb{E}(f(\bar{X}_T))$ induces the following weak error:

$$|\mathbb{E}f(X_T) - \mathbb{E}f(\bar{X}_T)| \leq \frac{C}{n}$$

with $C = C_{b, \sigma, T} > 0$ and where n is the number of time discretization steps.

(b) Also note that for every $p \geq 1$,

$$\mathbb{E}\left(\sup_{k=0, \dots, n} |\bar{X}_{t_k}|^p\right) < +\infty. \quad (6)$$

The estimation of quantities like (4) or (5) can be performed using Monte Carlo simulations. Nevertheless, an alternative to the Monte Carlo method can be to use cubature formulas produced by an optimal quantization approximation method, especially in small or medium dimension ($d \leq 4$ in the theory but in practice it may remain competitive with respect to the Monte Carlo method up to dimension $d = 10$, see [17]).

In fact, suppose that we have access to the optimal quantization or to some "good" (in a sense to be specified further on) quantizations $(\hat{X}_{t_k}^{\Gamma_k})_k$ (we will sometimes denote $\hat{X}_{t_k}^{\Gamma_k}$ by \hat{X}_{t_k} to simplify notations) of the process $(\bar{X}_{t_k})_k$ on the grids $\Gamma_k := \Gamma_k^{(N_k)} = \{x_1^k, \dots, x_{N_k}^k\}$ of size N_k (which will be called an N_k -quantizer), for $k = 0, \dots, n$. Suppose as well that we have access or have

computed (offline) the associated weights $\mathbb{P}(\widehat{X}_{t_k}^{\Gamma_k} = x_i^k)$, $i = 1, \dots, N_k$; $k = 0, \dots, n$ (which are the distributions of the $\widehat{X}_{t_k}^{\Gamma_k}$'s), and the transition probabilities $\widehat{p}_k^{ij} = \mathbb{P}(\widehat{X}_{t_{k+1}}^{\Gamma_{k+1}} = x_j^{k+1} | \widehat{X}_{t_k}^{\Gamma_k} = x_i^k)$ for every $k = 0, \dots, n-1$; $i = 1, \dots, N_k$; $j = 1, \dots, N_{k+1}$ (in other words, the conditional distributions $\mathcal{L}(\widehat{X}_{t_{k+1}}^{\Gamma_{k+1}} | \widehat{X}_{t_k}^{\Gamma_k})$). Then, using optimal quantization method, the expressions (4) and (5) can be estimated by

$$\mathbb{E}[f(\widehat{X}_{t_n}^{\Gamma_n})] = \sum_{i=1}^{N_n} f(x_i^n) \mathbb{P}(\widehat{X}_{t_n}^{\Gamma_n} = x_i^n)$$

and

$$\mathbb{E}[f(\widehat{X}_{t_{k+1}}^{\Gamma_{k+1}}) | \widehat{X}_{t_k}^{\Gamma_k} = x_i^k] = \sum_{j=1}^{N_{k+1}} \widehat{p}_k^{ij} f(x_j^{k+1}),$$

respectively. The remaining question to be solved is then to know how to get the optimal or at least “good” grids Γ_k , for every $k = 0, \dots, n$, their associated weights and transition probabilities. In a more general framework, as soon as the stochastic process $(\bar{X}_{t_k})_k$ (or the underlying diffusion process $(X_t)_{t \geq 0}$) can be simulated one may use stochastic gradient algorithm (CLVQ) or a randomized fixed point procedure (Lloyd) to compute the (hopefully almost) optimal grids and their associated weights or transition probabilities. In the special case of the one dimensional setting we can often use the Newton-Raphson’s algorithm in several situations of interest. This deterministic algorithm leads to more precise estimations and is dramatically faster than stochastic optimization methods.

To highlight the usefulness of our method, suppose for example that we aim to estimate the price of a Put option with a maturity T , strike K and a present value X_0 in a local volatility model where the dynamics of the stock price process evolves following the stochastic differential equation (called Pseudo-CEV in [11]):

$$dX_t = rX_t dt + \vartheta \frac{X_t^{\delta+1}}{\sqrt{1+X_t^2}} dW_t, \quad X_0 = x_0, \quad t \in [0, T], \quad (7)$$

where $\delta \in (0, 1)$ and $\vartheta \in (0, \vartheta]$, $\vartheta > 0$, and r stands for the interest rate. In this situation the solution at time T , X_T , is not known analytically and if we want to estimate the quantity of interest: $e^{-rT} \mathbb{E}(f(X_T))$, where $f(x) := \max(K - x, 0)$ is the (Lipschitz continuous) payoff function, we have first of all to discretize the process $(X_t)_{t \in [0, T]}$ as $(\bar{X}_{t_k})_{k=0, \dots, n}$, with $t_n = T$ (using e.g. the Euler scheme), and then estimate

$$e^{-rT} \mathbb{E}(f(\bar{X}_T))$$

by optimal quantization. The only way to get the optimal grids and the associated weights in this situation is to perform stochastic algorithms like the CLVQ (see e.g. [17]) or the Lloyd’s procedure (see e.g. [9, 19]), even in the one dimensional framework. However, these methods may be very time consuming. In this framework (as well as in the general local volatility model framework in dimension $d = 1$), our approach allows us to quantize the diffusion process in the Pseudo-CEV model using the Newton-Raphson algorithm to reduce dramatically the computational complexity of the search of optimal quantizers while increasing their computational precision with respect to commonly proposed algorithms. It is important to notice that the companion weights and the probability transitions associated to the quantized process are obtained by a closed formula so that the method involves by no means Monte Carlo simulations. On the other hand, a comparison with Monte Carlo simulation for the pricing of European options in a local volatility model also shows that the proposed method is more efficient (with respect to both computational precision and time complexity) than the Monte Carlo method.

Let us be more precise about our proposed method in the general setting where the diffusion $(X_t)_{t \in [0, T]}$ evolves following Equation (3). Let $(\bar{X}_{t_k})_{k=0, \dots, n}$ be the discrete Euler process, with step T/n , associated to the diffusion $(X_t)_{t \in [0, T]}$. Our aim is in practice to compute the quadratic optimal

quantizers (Γ_k) associated with the \bar{X}_k 's, for $k = 0, \dots, n$. Such a sequence (Γ_k) is defined for every $k = 0, \dots, n$ by

$$\Gamma_k \in \operatorname{argmin}\{\bar{D}_k(\Gamma), \Gamma \subset \mathbb{R}^d, \operatorname{card}(\Gamma) \leq N_k\}$$

where for every $k = 0, \dots, n$, the function $\bar{D}_k(\cdot)$ is called the distortion function associated to \bar{X}_{t_k} and is defined for every N_k -quantizer Γ_k by

$$\bar{D}_k(\Gamma_k) = \mathbb{E}|\bar{X}_{t_k} - \widehat{X}_{t_k}^{\Gamma_k}|^2 = \mathbb{E}(d(\bar{X}_{t_k}, \Gamma_k)^2).$$

Now, by conditioning with respect to \bar{X}_{t_k} , we observe that we can connect the distortion function $\bar{D}_{k+1}(\Gamma_{k+1}) = \mathbb{E}|\bar{X}_{t_{k+1}} - \widehat{X}_{t_{k+1}}^{\Gamma_{k+1}}|^2$ associated to $\bar{X}_{t_{k+1}}$ with the distribution of \bar{X}_{t_k} by introducing the Euler scheme operator as follows:

$$\begin{aligned} \bar{D}_{k+1}(\Gamma_{k+1}) &= \mathbb{E}(\mathbb{E}(d(\bar{X}_{t_{k+1}}, \Gamma_{k+1})^2 | \bar{X}_{t_k})) \\ &= \mathbb{E}(\mathbb{E}(d(\bar{X}_{t_{k+1}}, \Gamma_{k+1})^2 | \bar{X}_k)) \\ &= \mathbb{E}[d(\mathcal{E}_k(\bar{X}_{t_k}, Z_{k+1}), \Gamma_{k+1})^2] \end{aligned} \quad (8)$$

where $(Z_k)_k$ is an *i.i.d.* sequence of $\mathcal{N}(0; I_q)$ -distributed random vectors independent from \bar{X}_0 and for every $x \in \mathbb{R}^d$, the Euler operator $\mathcal{E}_k(x, Z_{k+1})$ is defined by

$$\mathcal{E}_k(x, Z_{k+1}) = x + \Delta b(t_k, x) + \sqrt{\Delta} \sigma(t_k, x) Z_{k+1}.$$

Now, here is how we construct the algorithm. Given the distribution of \bar{X}_0 , we quantize \bar{X}_0 and denote its quantization by $\widehat{X}_0^{\Gamma_0}$. We want now to quantize \bar{X}_{t_1} , which distribution is unknown. Keeping in mind Equation (8) and setting $\widetilde{X}_{t_1} := \mathcal{E}_0(\widehat{X}_0^{\Gamma_0}, Z_1)$, we may approximate the distortion function $\bar{D}_1(\Gamma_1)$ by

$$\widetilde{D}_1(\Gamma_1) = \mathbb{E}[d(\widetilde{X}_{t_1}, \Gamma_1)^2] = \mathbb{E}[d(\mathcal{E}_0(\widehat{X}_0^{\Gamma_0}, Z_1), \Gamma_1)^2].$$

We then define the marginal quantization of \bar{X}_{t_1} by $\widehat{X}_{t_1}^{\Gamma_1} = \operatorname{Proj}_{\Gamma_1}(\widetilde{X}_{t_1})$. This leads us to consider the sequence of marginal quantizations $(\widehat{X}_{t_k}^{\Gamma_k})_{k=0, \dots, n}$ of $(\bar{X}_{t_k}^{\Gamma_k})_{k=0, \dots, n}$, defined from the following recursion:

$$\begin{aligned} \widetilde{X}_0 &= \bar{X}_0 \\ \widehat{X}_{t_k}^{\Gamma_k} &= \operatorname{Proj}_{\Gamma_k}(\widetilde{X}_{t_k}) \quad \text{and} \quad \widetilde{X}_{t_{k+1}} = \mathcal{E}_k(\widehat{X}_{t_k}^{\Gamma_k}, Z_{k+1}) \\ (Z_k)_{k=1, \dots, n} &\text{ i.i.d., } \mathcal{N}(0; I_q)\text{-distributed, independent of } \bar{X}_0. \end{aligned}$$

From an analytical point of view, this approach raises some new challenging problems among which the estimation of the quadratic error bound $\|\bar{X}_{t_k} - \widehat{X}_{t_k}^{\Gamma_k}\|_2 := (\mathbb{E}|\bar{X}_{t_k} - \widehat{X}_{t_k}^{\Gamma_k}|_2^2)^{1/2}$, for every $k = 0, \dots, n$. We will show in particular that for any sequences of (quadratic) optimal quantizers Γ_k for $\bar{X}_{t_k}^{\Gamma_k}$, for every $k = 0, \dots, n-1$, the quantization error $\|\bar{X}_{t_k} - \widehat{X}_{t_k}^{\Gamma_k}\|_2$ is bounded by the cumulative quantization errors $\|\widetilde{X}_{t_i} - \widehat{X}_{t_i}^{\Gamma_i}\|_2$, for $i = 0, \dots, k$. Owing to the non-asymptotic bound for the quantization errors $\|\widetilde{X}_{t_i} - \widehat{X}_{t_i}^{\Gamma_i}\|_2$, known as Pierce's Lemma (which will be recalled further on) we precisely show that for every $k = 0, \dots, n$, for any $\eta \in]0, 1]$,

$$\|\bar{X}_k - \widehat{X}_k^{\Gamma_k}\|_2 \leq \sum_{\ell=0}^k a_\ell N_\ell^{-1/d},$$

where $a_\ell = a_\ell(b, \sigma, t_k, \Delta, x_0, L, \eta, d)$ is a positive real constant depending on the indicated parameters.

The paper is organized as follows. We recall first some basic facts about (regular) optimal quantization in Section 2. The marginal quantization method is described in Section 3. We give in this section

the induced quantization error. In section 4, we illustrate how to get the optimal grids using Newton-Raphson's algorithm and show how to estimate the associated weights and transition probabilities. The last section, Section 5, is devoted to numerical examples. We first compare the recursive marginal quantization of W_1 with its regular marginal quantization (see Section 2), where $(W_t)_{t \in [0,1]}$ stands for the Brownian motion and show the numerical performance of the marginal quantization method with respect to the regular quantization method. Secondly, we use the marginal quantization method for the pricing of an European Put option in a local volatility model (as well as in the Black-Scholes model) and compare the results with those obtained from the Monte Carlo method.

NOTATIONS. We denote by $\mathcal{M}(d, q, \mathbb{R})$, the set of $d \times q$ real value matrices. If $A = [a_{ij}] \in \mathcal{M}(d, q, \mathbb{R})$, A^* denotes its transpose and we define the norm $\|A\| := \sqrt{\text{Tr}(AA^*)} = (\sum_{i,j} a_{ij}^2)^{1/2}$, where $\text{Tr}(M)$ stands for the trace of M , for $M \in \mathcal{M}(d, d, \mathbb{R})$. For every $f : \mathbb{R}^d \rightarrow \mathcal{M}(d, q, \mathbb{R})$, we will set $[f]_{\text{Lip}} = \sup_{x \neq y} \frac{\|f(x) - f(y)\|}{|x - y|}$. For $x, y \in \mathbb{R}$, $x \vee y = \max(x, y)$.

2 Background on optimal quantization

Let $(\Omega, \mathcal{A}, \mathbb{P})$ be a probability space and let $X : (\Omega, \mathcal{A}, \mathbb{P}) \rightarrow \mathbb{R}^d$ be a random variable with distribution \mathbb{P}_X . The L^r -optimal quantization problem at level N for the random vector X (or for the distribution \mathbb{P}_X) consists in finding the best approximation of X by a Borel function $\pi(X)$ of X taking at most N values. Assuming that $X \in L^r(\mathbb{P})$, we associate to every Borel function $\pi(X)$ taking at most N values, the L^r -mean error $\|X - \pi(X)\|_r$ measuring the distance between the two random vectors X and $\pi(X)$ w.r.t. the mean L^r -norm, where $\|X\|_r := (\mathbb{E}|X|^r)^{1/r}$ and $|\cdot|$ denotes an arbitrary norm on \mathbb{R}^d . Then finding the best approximation of X by a Borel function of X taking at most N values turns out to solve the following minimization problem:

$$e_{N,r}(X) = \inf \{ \|X - \pi(X)\|_r, \pi : \mathbb{R}^d \rightarrow \Gamma, \Gamma \subset \mathbb{R}^d, |\Gamma| \leq N \},$$

where $|A|$ stands for the cardinality of A , for $A \subset \mathbb{R}^d$. Now, let $\Gamma = \{x_1, \dots, x_N\} \subset \mathbb{R}^d$ be a codebook of size N (also called an N -quantizer or a grid of size N) and define a Voronoi partition $C_i(\Gamma)_{i=1, \dots, N}$ of \mathbb{R}^d , which is a Borel partition of \mathbb{R}^d satisfying for every $i \in \{1, \dots, N\}$,

$$C_i(\Gamma) \subset \{x \in \mathbb{R}^d : |x - x_i| = \min_{j=1, \dots, N} |x - x_j|\}.$$

Consider the Voronoi quantization of X (simply called quantization of X) by the N -quantizer Γ defined by

$$\widehat{X}^\Gamma = \sum_{i=1}^N x_i \mathbf{1}_{\{X \in C_i(\Gamma)\}}.$$

Then, for any Borel function $\pi : \mathbb{R}^d \rightarrow \Gamma = \{x_1, \dots, x_N\}$ we have

$$|X - \pi(X)| \geq \min_{i=1, \dots, N} d(X, x_i) = d(X, \Gamma) = |X - \widehat{X}^\Gamma| \quad \mathbb{P} \text{ a.s.}$$

so that the optimal L^r -mean quantization error $e_{N,r}(X)$ reads

$$\begin{aligned} e_{N,r}(X) &= \inf \{ \|X - \widehat{X}^\Gamma\|_r, \Gamma \subset \mathbb{R}^d, |\Gamma| \leq N \} \\ &= \inf_{\substack{\Gamma \subset \mathbb{R}^d \\ |\Gamma| \leq N}} \left(\int_{\mathbb{R}^d} d(z, \Gamma)^r d\mathbb{P}_X(z) \right)^{1/r}. \end{aligned} \quad (9)$$

Recall that for every $N \geq 1$, the infimum in (9) is attained at least one codebook. Any N -quantizer realizing this infimum is called an L^r -optimal N -quantizer. Moreover, when $|\text{supp}(\mathbb{P}_X)| \geq N$ then any L^r -mean optimal N -quantizer has exactly size N (see [10] or [13]). On the other hand, the quantization error, $e_{N,r}(X)$, decreases to zero as the grid size N goes to infinity and its rate of convergence is ruled by the so-called Zador Theorem recalled below. There also is a non-asymptotic upper bound for optimal quantizers. It is called Pierce Lemma (we recall it below for the quadratic case) and will allow us to put a finishing touch to the proof of the main result of the paper, stated in Theorem 3.1.

Theorem 2.1. (a) (**Zador**, see [10]). Let X be an \mathbb{R}^d -valued random vector such that $\mathbb{E}|X|^{r+\eta} < +\infty$ for some $\eta > 0$ and let $\mathbb{P}_X = f \cdot \lambda_d + P_s$ be the Lebesgue decomposition of \mathbb{P}_X with respect to the Lebesgue measure λ_d and P_s denotes its singular part. Then

$$\lim_{N \rightarrow +\infty} N^{\frac{1}{d}} e_{N,r}(P) = \tilde{Q}_r(\mathbb{P}_X) \quad (10)$$

with

$$\begin{aligned} \tilde{Q}_r(\mathbb{P}_X) &= \tilde{J}_{r,d} \left(\int_{\mathbb{R}^d} f^{\frac{d}{d+r}} d\lambda_d \right)^{\frac{1}{r} + \frac{1}{d}} = \tilde{J}_{r,d} \|f\|_{\frac{d}{d+r}}^{1/r} \in [0, +\infty), \\ \tilde{J}_{r,d} &= \inf_{N \geq 1} N^{\frac{1}{d}} e_{N,r}(U([0, 1]^d)) \in (0, +\infty), \end{aligned}$$

where $U([0, 1]^d)$ denotes the uniform distribution over the hypercube $[0, 1]^d$.

(b) (**Pierce**, see [10, 12]). Let $\eta > 0$. There exists a universal constant $K_{2,d,\eta}$ such that for every random vector $X : (\Omega, \mathcal{A}, \mathbb{P}) \rightarrow \mathbb{R}^d$,

$$\inf_{|\Gamma| \leq N} \|X - \hat{X}^\Gamma\|_2 \leq K_{2,d,\eta} \sigma_{2,\eta}(X) N^{-\frac{1}{d}}, \quad (11)$$

where

$$\sigma_{2,\eta}(X) = \inf_{\zeta \in \mathbb{R}^d} \|X - \zeta\|_{2+\eta} \leq +\infty.$$

We will call $\tilde{Q}_r(\mathbb{P}_X)$ the Zador's constant associated to X . From the Numerical Probability point of view, finding an optimal N -quantizer Γ may be a challenging task. In practice (we will only consider the quadratic case, i.e. $r = 2$ for numerical implementations) we are sometimes led to find some "good" quantizations \hat{X}^Γ which are close to X in distribution, so that for every continuous function $f : \mathbb{R}^d \rightarrow \mathbb{R}$, we can approximate $\mathbb{E}f(X)$ by

$$\mathbb{E}f(\hat{X}^\Gamma) = \sum_{i=1}^N p_i f(x_i), \quad (12)$$

where $p_i = \mathbb{P}(\hat{X}^\Gamma = x_i)$. We recall below the stationarity property for a quantizer.

Definition 2.1. An N -quantizer $\Gamma = \{x_1, \dots, x_N\}$ inducing the quantization \hat{X}^Γ of X is stationary if

$$\forall i \neq j, \quad x_i \neq x_j, \quad \mathbb{P}(X \in \cup_i \partial C_i(\Gamma)) = 0, \quad i = 1, \dots, N$$

and

$$\mathbb{E}(X | \hat{X}^\Gamma) = \hat{X}^\Gamma. \quad (13)$$

We define the distortion function by

$$D_{N,2}(\Gamma) = \mathbb{E}|X - \widehat{X}^\Gamma|^2 = \int_{\mathbb{R}^d} d(x, \Gamma)^2 d\mathbb{P}_X(x) = \sum_{i=1}^N \int_{C_i(\Gamma)} |x - x_i|^2 d\mathbb{P}_X(x), \quad (14)$$

so that

$$e_{N,2}^2(X) = \inf_{\Gamma \in (\mathbb{R}^d)^N} D_{N,2}(\Gamma).$$

By definition, a stationary quantizer $\Gamma = \{x_1, \dots, x_N\}$ is in fact an N -quantizer satisfying the stationary equality:

$$\nabla D_{N,2}(\Gamma) = 0.$$

The following result justifies the interchange of the differentiation and the integral leading to (29) when differentiating (14), see [10].

Proposition 2.2. *The function $D_{N,2}$ is differentiable at any N -tuple $\Gamma \in (\mathbb{R}^d)^N$ having pairwise distinct components and such that $\mathbb{P}(X \in \cup_i \partial C_i(\Gamma)) = 0$. Furthermore, we have*

$$\nabla D_{N,2}(\Gamma) = 2 \left(\int_{C_i(\Gamma)} (x_i - x) d\mathbb{P}_X(x) \right)_{i=1, \dots, N}. \quad (15)$$

For numerical implementations, the search of stationary quantizers is based on zero search recursive procedures like Newton-Raphson algorithm for real valued random variables, and some algorithms like Lloyd's I algorithms (see e.g. [9, 19]), the Competitive Learning Vector Quantization (CLVQ) algorithm (see [9]) or stochastic algorithms (see [16]) in the multidimensional framework. Optimal quantization grids associated to multivariate Gaussian random vectors can be downloaded on the website www.quantize.math-fi.com.

When approximating $\mathbb{E}f(X)$ by $\mathbb{E}f(\widehat{X}^\Gamma)$ where Γ is an N -quantizer, the resulting error may be bounded by the squared quantization error $\mathbb{E}|X - \widehat{X}^\Gamma|^2$, depending on the regularity of the function f . We next recall some error bounds induced from the approximation of $\mathbb{E}f(X)$ by (12) (we refer to [17] for further detail).

- (a) Let Γ be a stationary quantizer and f be a Borel function on \mathbb{R}^d . If f is a convex function then

$$\mathbb{E}f(\widehat{X}^\Gamma) \leq \mathbb{E}f(X). \quad (16)$$

- (b) Lipschitz functions:

- If f is Lipschitz continuous then for any N -quantizer Γ we have

$$|\mathbb{E}f(X) - \mathbb{E}f(\widehat{X}^\Gamma)| \leq [f]_{\text{Lip}} \|X - \widehat{X}^\Gamma\|_2,$$

where

$$[f]_{\text{Lip}} := \sup_{x \neq y} \frac{|f(x) - f(y)|}{|x - y|}.$$

- Let $\theta : \mathbb{R}^d \rightarrow \mathbb{R}_+$ be a nonnegative convex function such that $\theta(X) \in L^2(\mathbb{P})$. If f is locally Lipschitz with at most θ -growth, i.e. $|f(x) - f(y)| \leq [f]_{\text{Lip}} |x - y| (\theta(x) + \theta(y))$ then $f(X) \in L^1(\mathbb{P})$ and

$$|\mathbb{E}f(X) - \mathbb{E}f(\widehat{X}^\Gamma)| \leq 2[f]_{\text{Lip}} \|X - \widehat{X}^\Gamma\|_2 \|\theta(X)\|_2.$$

- (c) Differentiable functionals: if f is differentiable on \mathbb{R}^d with an α -Hölder gradient ∇f ($\alpha \in [0, 1]$), then for any stationary N -quantizer Γ ,

$$|\mathbb{E}f(X) - \mathbb{E}f(\widehat{X}^\Gamma)| \leq [\nabla f]_\alpha \|X - \widehat{X}^\Gamma\|_2^{1+\alpha}.$$

3 Recursive marginal quantization of a discrete stochastic diffusion process

Let $(X_t)_{t \geq 0}$ be a stochastic process taking values in a d -dimensional Euclidean space \mathbb{R}^d and solution to the stochastic differential equation:

$$dX_t = b(t, X_t)dt + \sigma(t, X_t)dW_t, \quad X_0 = x_0 \in \mathbb{R}^d, \quad (17)$$

where W is a standard q -dimensional Brownian motion starting at 0 and where $b : [0, T] \times \mathbb{R}^d \rightarrow \mathbb{R}^d$ and the matrix diffusion coefficient function $\sigma : [0, T] \times \mathbb{R}^d \rightarrow \mathcal{M}(d, q, \mathbb{R})$ are measurable and satisfy the global Lipschitz and linear growth conditions: for every $t \in [0, T]$,

$$|b(t, x) - b(t, y)| \leq [b]_{\text{Lip}}|x - y| \quad (18)$$

$$\|\sigma(t, x) - \sigma(t, y)\| \leq [\sigma]_{\text{Lip}}|x - y| \quad (19)$$

$$|b(t, x)| \leq L(1 + |x|) \quad \text{and} \quad \|\sigma(t, x)\| \leq L(1 + |x|). \quad (20)$$

$L > 0$. This guarantees the existence of a strong solution of (17). We also suppose that the matrix σ is positive definite. Throughout the paper we will suppose that \mathbb{R}^d is equipped with the canonical Euclidean norm.

3.1 The algorithm

Consider the Euler scheme of the process $(X_t)_{t \geq 0}$ starting from $\bar{X}_0 = X_0$:

$$\bar{X}_{t_{k+1}} = \bar{X}_{t_k} + \Delta b(t_k, \bar{X}_{t_k}) + \sigma(t_k, \bar{X}_{t_k})(W_{t_{k+1}} - W_{t_k}),$$

where $t_k = \frac{kT}{n}$, for every $k \in \{0, \dots, n\}$.

NOTATIONS SIMPLIFICATION. To alleviate notations, we set

$$Y_k := Y_{t_k} \quad (\text{for any process } Y \text{ evaluated at time } t_k)$$

$$b_k(x) := b(t_k, x), \quad x \in \mathbb{R}^d$$

$$\sigma_k(x) = \sigma(t_k, x), \quad x \in \mathbb{R}^d.$$

Recall that the distortion function \bar{D}_k associated to \bar{X}_k may be written for every $k = 0, \dots, n-1$, as

$$\bar{D}_{k+1}(\Gamma_{k+1}) = \mathbb{E}[d(\mathcal{E}_k(\bar{X}_k, Z_{k+1}), \Gamma_{k+1})^2]$$

where

$$\mathcal{E}_k(x, z) := x + \Delta b(t_k, x) + \sqrt{\Delta} \sigma(t_k, x)z, \quad x \in \mathbb{R}^d, \quad z \in \mathbb{R}^q.$$

Now, supposing that \bar{X}_0 has already been quantized and setting $\tilde{X}_1 = \mathcal{E}_0(\hat{X}_0^{\Gamma_0}, Z_1)$, we may approximate the distortion function \bar{D}_1 by

$$\begin{aligned} \tilde{D}_1(\Gamma_1) &:= \mathbb{E}[d(\tilde{X}_1, \Gamma_1)^2] \\ &= \mathbb{E}[d(\mathcal{E}_0(\hat{X}_0^{\Gamma_0}, Z_1), \Gamma_1)^2] \\ &= \sum_{i=1}^{N_0} \mathbb{E}[d(\mathcal{E}_0(x_i^0, Z_1), \Gamma_1)^2] \mathbb{P}(\hat{X}_0^{\Gamma_0} = x_i^0). \end{aligned}$$

This allows us (as it is already said in the introduction) to consider the sequence of (marginal) quantizations $(\hat{X}_k^{\Gamma_k})_{k=0, \dots, n}$ defined from the following recursion:

$$\hat{X}_k^{\Gamma_k} = \text{Proj}_{\Gamma_k}(\tilde{X}_k) \quad \text{and} \quad \tilde{X}_{k+1} = \mathcal{E}_k(\hat{X}_k^{\Gamma_k}, Z_{k+1})$$

where $\tilde{X}_0 = \bar{X}_0$ and $(Z_k)_{k=1, \dots, n}$ is *i.i.d.*, $\mathcal{N}(0; I_q)$ -distributed, independent of \bar{X}_0 .

3.2 The error analysis

Our aim is now to compute the quantization error bound $\|\bar{X}_T - \hat{X}_T\|_2 := \|\bar{X}_n - \hat{X}_n^{\Gamma_n}\|_2$. The analysis of this error bound will be the subject of the following theorem, which is the main result of the paper. Keep in mind that $x_0 = X_0 = \tilde{X}_0$.

Theorem 3.1. *Let the coefficients b, σ satisfy the assumptions (18), (19) and (20). Let for every $k = 0, \dots, n$, Γ_k be a quadratic optimal quantizer for \tilde{X}_k at level N_k . Then, for every $k = 0, \dots, n$, for any $\eta \in]0, 1]$,*

$$\|\bar{X}_k - \hat{X}_k^{\Gamma_k}\|_2 \leq K_{2,d,\eta} \sum_{\ell=0}^k a_\ell(b, \sigma, t_k, \Delta, x_0, L, 2 + \eta) N_\ell^{-1/d}, \quad (21)$$

where for every $p \in (2, 3]$,

$$a_\ell(b, \sigma, t_k, \Delta, x_0, L, p) := e^{C_{b,\sigma} \frac{(t_k - t_\ell)}{p}} \left[e^{(\kappa_p + K_p)t_\ell} |x_0|^p + \frac{e^{\kappa_p \Delta} L + K_p}{\kappa_p + K_p} (e^{(\kappa_p + K_p)t_\ell} - 1) \right]^{\frac{1}{p}},$$

with $C_{b,\sigma} = [b]_{\text{Lip}} + \frac{1}{2}[\sigma]_{\text{Lip}}^2$, $K_{2,d,\eta}$ is a universal constant defined in Equation (11) and given in [12];

$$\kappa_p := \left(\frac{(p+1)(p-2)}{2} + 2pL \right) \text{ and } K_p := 2^{p-1} L^p \left(1 + p + \Delta^{\frac{p}{2}-1} \right) \mathbb{E}|Z|^p, \quad Z \sim \mathcal{N}(0; I_d).$$

Let us make the following remarks.

Remark 3.1. It is important to notice that the constants $a_\ell(\cdot, t_k, \cdot, \cdot, \cdot, \cdot, p)$ do not explode when n goes to infinity and we have

$$\max_{k,\ell=0,\dots,n} a_\ell(\cdot, t_k, \cdot, \cdot, \cdot, \cdot, p) \leq e^{C_{b,\sigma} \frac{T}{p}} \left[e^{(\kappa_p + K_p)T} |x_0|^p + \frac{e^{\kappa_p T} L + K_p}{\kappa_p + K_p} (e^{(\kappa_p + K_p)T} - 1) \right]^{\frac{1}{p}}.$$

We also remark that $\kappa_p \leq 2(1+p)L$.

Before dealing with the proof of the theorem, we give below a lemma which will be used to complete the proof of the theorem. The proof of the lemma is postponed to the appendix.

Lemma 3.2. *Let the coefficients b, σ of the diffusion satisfy the assumptions (19) and (20). Then, for every $p \in (2, 3]$, for every $k = 0, \dots, n$,*

$$\mathbb{E}|\tilde{X}_k|^p \leq e^{(\kappa_p + K_p)t_k} |x_0|^p + \frac{e^{\kappa_p \Delta} L + K_p}{\kappa_p + K_p} (e^{(\kappa_p + K_p)t_k} - 1), \quad (22)$$

where K_p and κ_p are defined in Theorem 3.1.

Let us prove the theorem.

Proof (of Theorem 3.1). First we note that for every $k = 0, \dots, n$,

$$\|\bar{X}_k - \hat{X}_k\|_2 \leq \|\bar{X}_k - \tilde{X}_k\|_2 + \|\tilde{X}_k - \hat{X}_k^{\Gamma_k}\|_2. \quad (23)$$

Let us control the first term of the right hand side of the above equation. To this end, we first note that, for every $k = 0, \dots, n$, the function $\mathcal{E}_k(\cdot, Z_{k+1})$ is Lipschitz w.r.t. the L^2 -norm: in fact, for every $x, x' \in \mathbb{R}^d$,

$$\begin{aligned} \mathbb{E}|\mathcal{E}_k(x, Z_{k+1}) - \mathcal{E}_k(x', Z_{k+1})|^2 &\leq (1 + \Delta(2[b_k(\cdot)]_{\text{Lip}} + [\sigma_k(\cdot)]_{\text{Lip}}^2) + \Delta^2[b_k(\cdot)]_{\text{Lip}}^2) |x - x'|^2 \\ &\leq (1 + \Delta(2[b]_{\text{Lip}} + [\sigma]_{\text{Lip}}^2) + \Delta^2[b]_{\text{Lip}}^2) |x - x'|^2 \\ &\leq (1 + \Delta C_{b,\sigma})^2 |x - x'|^2 \\ &\leq e^{2\Delta C_{b,\sigma}} |x - x'|^2, \end{aligned}$$

where $C_{b,\sigma} = [b]_{\text{Lip}} + \frac{1}{2}[\sigma]_{\text{Lip}}^2$ does not depend on n . Then, it follows that for every $\ell = 0, \dots, k-1$,

$$\begin{aligned} \|\bar{X}_{\ell+1} - \tilde{X}_{\ell+1}\|_2 &= \|\mathcal{E}_\ell(\bar{X}_\ell, Z_{\ell+1}) - \mathcal{E}_\ell(\hat{X}_\ell^{\Gamma_\ell}, Z_{\ell+1})\|_2 \\ &\leq e^{\Delta C_{b,\sigma}} \|\bar{X}_\ell - \hat{X}_\ell^{\Gamma_\ell}\|_2 \\ &\leq e^{\Delta C_{b,\sigma}} \|\bar{X}_\ell - \tilde{X}_\ell\|_2 + e^{\Delta C_{b,\sigma,T}} \|\tilde{X}_\ell - \hat{X}_\ell^{\Gamma_\ell}\|_2. \end{aligned} \quad (24)$$

Then, we show by a backward induction using (23) and (24) that

$$\|\bar{X}_k - \tilde{X}_k\|_2 \leq \sum_{\ell=0}^k e^{(k-\ell)\Delta C_{b,\sigma}} \|\tilde{X}_\ell - \hat{X}_\ell^{\Gamma_\ell}\|_2.$$

Now, one deduces from Lemma 11 and then, from Lemma 3.2 that, for every $k = 0, \dots, n$, for any $\eta > 0$

$$\begin{aligned} \|\bar{X}_k - \hat{X}_k\|_2 &\leq K_{2,d,\eta} \sum_{\ell=0}^k e^{(k-\ell)\Delta C_{b,\sigma}} \sigma_{2,\eta}(\tilde{X}_\ell) N_\ell^{-1/d} \\ &\leq K_{2,d,\eta} \sum_{\ell=0}^k e^{(k-\ell)\Delta C_{b,\sigma}} \|\tilde{X}_\ell\|_{2+\eta} N_\ell^{-1/d} \\ &\leq K_{2,d,\eta} \sum_{\ell=0}^k (a_\ell(b, \sigma, t_k, \Delta, x_0, L, 2 + \eta))^{1/(2+\eta)} N_\ell^{-1/d}, \end{aligned}$$

which is the announced result. \square

Remark 3.2. (a) When we consider the upper bound of Equation (21), a natural question is to determine how to dispatch optimally the sizes N_0, \dots, N_n (for a fixed mesh of length n) of the quantization grids when we wish to use a total “budget” $N = N_0 + \dots + N_n$ of elementary quantizers (with $N_k \geq 1$, for every $k = 0, \dots, n$). This amounts to solving the minimization problem

$$\min_{N_0 + \dots + N_n = N} \sum_{\ell=0}^n a_\ell N_\ell^{-1/d}$$

where $a_\ell = a_\ell(b, \sigma, t_n, \Delta, x_0, L, 2 + \eta)$. This leads (see e.g. [1]) to the following optimal dispatching: $N_0 = 1$ (since X_0 is not random) and for every $\ell = 1, \dots, n$,

$$N_\ell = \left\lfloor \frac{a_\ell^{\frac{d}{d+1}}}{\sum_{k=0}^n a_k^{\frac{d}{d+1}}} N \right\rfloor \vee 1,$$

so that Equation (21) becomes (for $k = n$)

$$\|\bar{X}_n - \hat{X}_n^{\Gamma_n}\|_2 \leq K_{2,d,\eta} N^{-1/d} \left(\sum_{\ell=0}^n a_\ell^{\frac{d}{d+1}} \right)^{1+1/d}$$

and using the convexity inequality leads to

$$\begin{aligned} \|\bar{X}_n - \hat{X}_n^{\Gamma_n}\|_2 &\leq K_{2,d,\eta} N^{-1/d} (n+1)^{1+\frac{1}{d}} \left(\sum_{\ell=0}^n \frac{1}{n+1} a_\ell^{\frac{d}{d+1}} \right)^{1+1/d} \\ &\leq K_{2,d,\eta} N^{-1/d} (n+1)^{1/d} \sum_{\ell=0}^n a_\ell. \end{aligned}$$

(b) If we assign $N_k = \bar{N} := N/(n+1)$ points to each grid Γ_k , the error bound in Theorem 3.1 leads to

$$\|\bar{X}_n - \widehat{X}_n^{\Gamma_n}\|_2 \leq K_{2,d,\eta} \left(\frac{n+1}{N}\right)^{1/d} \sum_{\ell=0}^n a_\ell.$$

4 Computation of the marginal quantizers

We focus now on the numerical computation of the quadratic optimal quantizers of the marginal random variable $\tilde{X}_{t_{k+1}}$ given the probability distribution function of \tilde{X}_{t_k} . Such a task requires the use of some algorithms like the CLVQ algorithm, Lloyd's algorithms (both requiring the computation of the gradient of the distortion function) or Newton-Raphson's algorithm (especially for the one-dimensional setting) which involves the gradient and the Hessian matrix of the distortion (we refer to [17] for more details).

Let $\widehat{X}_k^{\Gamma_k}$ be the quantization of \tilde{X}_k induced by the grid Γ_k and let $\tilde{D}_k(\Gamma_k) = \|\tilde{X}_k - \widehat{X}_k^{\Gamma_k}\|_2$ be the associated distortion function, for $k = 0, \dots, n$. Our aim is to compute the (at least locally) optimal quadratic quantization grids $(\Gamma_k)_{k=0, \dots, n}$ associated with the \tilde{X}_k 's, $k = 0, \dots, n$. Such a sequence of grids $(\Gamma_k)_{k=0, \dots, n}$ is defined for every $k = 0, \dots, n$ by

$$\Gamma_k \in \operatorname{argmin}\{\tilde{D}_k(\Gamma), \Gamma \subset \mathbb{R}^d, \operatorname{card}(\Gamma) \leq N_k\}. \quad (25)$$

Recall that the sequence of (marginal) quantizations $(\widehat{X}_k)_{k=0, \dots, n}$ is defined by the following induction:

$$\tilde{X}_0 = \bar{X}_0 \quad (26)$$

$$\widehat{X}_k = \operatorname{Proj}_{\Gamma_k}(\tilde{X}_k) \quad \text{and} \quad \tilde{X}_{k+1} = \mathcal{E}_k(\widehat{X}_k, Z_{k+1}) \quad (27)$$

$$Z_k \stackrel{\text{i.i.d.}}{\sim} \mathcal{N}(0; I_q), k = 1, \dots, n, \quad \text{and} \quad (Z_k)_k \text{ is independent from } \bar{X}_0. \quad (28)$$

Supposing that \tilde{X}_k has already been quantized, we have for every $k = 0, \dots, n-1$,

$$\begin{aligned} \tilde{D}_{k+1}(\Gamma_{k+1}) &= \mathbb{E}[d(\mathcal{E}_k(\widehat{X}_k, Z_{k+1}), \Gamma_{k+1})^2] \\ &= \sum_{i=1}^{N_k} \mathbb{E}[d(\mathcal{E}_k(x_i^{N_k}, Z_{k+1}), \Gamma_{k+1})^2] \mathbb{P}(\widehat{X}_k = x_i^{N_k}). \end{aligned}$$

Then, owing to Proposition 2.2, the distortion function $\tilde{D}_{k+1}(\Gamma_{k+1})$ is continuously differentiable as a function of the N_{k+1} -quantizer Γ_{k+1} (having pairwise distinct components) and its gradient is given by

$$\nabla \tilde{D}_{k+1}(x^{N_{k+1}}) = 2 \left[\sum_{i=1}^{N_k} \mathbb{E} \left(\mathbf{1}_{\{\mathcal{E}_k(x_i^{N_k}, Z_{k+1}) \in C_j(\Gamma_{k+1})\}} (x_j^{k+1} - \mathcal{E}_k(x_i^{N_k}, Z_{k+1})) \right) \mathbb{P}(\widehat{X}_k = x_i^{N_k}) \right]_{j=1, \dots, N_{k+1}}.$$

Remark 4.1. a) If Γ_{k+1} is a quadratic optimal N_{k+1} -quantizer for \tilde{X}_{k+1} and if $\widehat{X}_{k+1}^{\Gamma_{k+1}}$ denotes the quantization of \tilde{X}_{k+1} on the grid Γ_{k+1} . Then Γ_{k+1} is a stationary quantizer, i.e.,

$$\nabla \tilde{D}_{k+1}(\Gamma_{k+1}) = 0. \quad (29)$$

Equivalently, we have for every $j = 1, \dots, N_{k+1}$,

$$x_j^{N_{k+1}} = \frac{\sum_{i=1}^{N_k} \mathbb{E} \left(\mathcal{E}_k(x_i^{N_k}, Z_{k+1}) \mathbf{1}_{\{\mathcal{E}_k(x_i^{N_k}, Z_{k+1}) \in C_j(\Gamma_{k+1})\}} \right) \mathbb{P}(\widehat{X}_k = x_i^{N_k})}{\sum_{i=1}^{N_k} \mathbb{P}(\mathcal{E}_k(x_i^{N_k}, Z_{k+1}) \in C_j(\Gamma_{k+1})) \mathbb{P}(\widehat{X}_k = x_i^{N_k})}. \quad (30)$$

This also means that

$$\mathbb{E}\left(\tilde{X}_{k+1}|\hat{X}_{k+1}\right) = \hat{X}_{k+1}.$$

b) In higher dimension $d \geq 2$, equations (29) and (30) allow us to compute stationary quantizers for \tilde{X}_{k+1} using stochastic algorithms and Lloyd's type algorithms, given that \tilde{X}_k has already been quantized.

As mentioned in [17], the usual CLVQ or Lloyd's companion algorithms become quickly untractable when the dimension $d \geq 2$ due to the fact that we have to compute d -dimension integrals on Voronoi cells. Moreover, in our setting the complexity of these algorithms will increase since we have to compute additional d -dimensional integrals. For these reasons, we will restrict our analysis to the one-dimensional setting where we will use the Newton-Raphson algorithm in \mathbb{R}^{N_k} to perform recursively quadratic optimal quantizers of the marginals \tilde{X}_k given the distribution of X_0 .

4.1 The one dimensional setting

For $k \in \{0, \dots, n\}$, let $\nabla \tilde{D}_k(\Gamma_k)$ and $\nabla^2 \tilde{D}_k(\Gamma_k)$ denote respectively the gradient vector and the hessian matrix of the distortion function \tilde{D}_k . To simplify notations set, for $k = 0, \dots, n-1$ and for $j = 1, \dots, N_{k+1}$,

$$x_{j-1/2}^{k+1} = \frac{x_j^{k+1} + x_{j-1}^{k+1}}{2}, \quad x_{j+1/2}^{k+1} = \frac{x_j^{k+1} + x_{j+1}^{k+1}}{2}, \quad \text{with } x_{1/2}^{k+1} = -\infty, x_{N_{k+1}+1/2}^{k+1} = +\infty,$$

and let

$$x_{k+1,j-}(x) := \frac{x_{j-1/2}^{k+1} - m_k(x)}{v_k(x)} \quad \text{and} \quad x_{k+1,j+}(x) := \frac{x_{j+1/2}^{k+1} - m_k(x)}{v_k(x)},$$

where $v_k(x) = \sqrt{\Delta} \sigma_k(x)$ and $m_k(x) = x + \Delta b_k(x)$. We also denote by $\Phi_0(\cdot)$ and $\Phi'_0(\cdot)$ the probability distribution function and the cumulative distribution function, respectively, of the standard Gaussian distribution.

4.1.1 Computing marginal quantizers with Newton-Raphson algorithm

Our procedure is recursive and we suppose that Γ_k (quantizer for \tilde{X}_k) has been computed as well as the companion weights: $\mathbb{P}(\tilde{X}_{t_k} \in C_i(\Gamma_k)), i = 1, \dots, N_k$. Therefore, using the Newton-Raphson zero search, a zero of the gradient can be computed via the following recursive procedure starting from a given initial point $\Gamma_{k+1}^{(0)} \in \mathbb{R}^{N_{k+1}}$:

$$\Gamma_{k+1}^{(\ell+1)} = \Gamma_{k+1}^{(\ell)} - (\nabla^2 \tilde{D}_{k+1}(\Gamma_{k+1}^{(\ell)}))^{-1} \nabla \tilde{D}_{k+1}(\Gamma_{k+1}^{(\ell)}), \quad \ell = 0, 1, \dots, L-1, \quad (31)$$

where the components of $\nabla \tilde{D}_{k+1}(\Gamma_{k+1})$ are given for every $\Gamma_{k+1}^{(\ell)} := \Gamma_{k+1} = (x_1^{k+1}, \dots, x_{N_{k+1}}^{k+1})$, $\ell = 0, \dots, L-1$ (where L is the number of iterations of the Newton-Raphson procedure), and for every $j = 1, \dots, N_{k+1}$, by

$$\begin{aligned} \frac{\partial \tilde{D}_{k+1}(\Gamma_{k+1})}{\partial x_j^{k+1}} = & \sum_{i=1}^{N_k} \left\{ (x_j^{k+1} - m_k(x_i^k)) \left(\Phi'_0(x_{k+1,j+}(x_i^k)) - \Phi'_0(x_{k+1,j-}(x_i^k)) \right) \right. \\ & \left. + v_k(x_i^k) \left(\Phi_0(x_{k+1,j+}(x_i^k)) - \Phi_0(x_{k+1,j-}(x_i^k)) \right) \right\} \mathbb{P}(\tilde{X}_k \in C_i(\Gamma_k)). \end{aligned}$$

The diagonal terms of the Hessian matrix $\nabla^2 \tilde{D}_{k+1}(\Gamma_{k+1})$ are given by:

$$\begin{aligned} \frac{\partial^2 \tilde{D}_{k+1}(\Gamma_{k+1})}{\partial^2 x_j^{k+1}} &= \sum_{i=1}^{N_k} \left[\Phi'_0(x_{k+1,j+}(x_i^k)) - \Phi'_0(x_{k+1,j-}(x_i^k)) \right. \\ &\quad - \frac{1}{4v_k(x_i^k)} \Phi_0(x_{k+1,j+}(x_i^k))(x_{j+1}^{k+1} - x_j^{k+1}) \\ &\quad \left. - \frac{1}{4v_k(x_i^k)} \Phi_0(x_{k+1,j-}(x_i^k))(x_j^{k+1} - x_{j-1}^{k+1}) \right] \mathbb{P}(\tilde{X}_k \in C_i(\Gamma_k)) \end{aligned}$$

and its sub-diagonal terms are

$$\frac{\partial^2 \tilde{D}_{k+1}(\Gamma_{k+1})}{\partial x_j^{k+1} \partial x_{j-1}^{k+1}} = -\frac{1}{4} \sum_{i=1}^{N_k} \frac{1}{v_k(x_i^k)} (x_j^{k+1} - x_{j-1}^{k+1}) \Phi_0(x_{k+1,j-}(x_i^k)) \mathbb{P}(\tilde{X}_k \in C_i(\Gamma_k)).$$

The super-diagonals terms are

$$\frac{\partial^2 \tilde{D}_{k+1}(\Gamma_{k+1})}{\partial x_j^{k+1} \partial x_{j+1}^{k+1}} = -\frac{1}{4} \sum_{i=1}^{N_k} \frac{1}{v_k(x_i^k)} (x_j^{k+1} - x_{j+1}^{k+1}) \Phi_0(x_{k+1,j+}(x_i^k)) \mathbb{P}(\tilde{X}_k \in C_i(\Gamma_k)).$$

A similar idea combining (vector or functional) optimal quantization with Newton-Raphson zero search procedure is used in [8] in a variance reduction context as an alternative and robust method to simulation based recursive importance sampling procedure to estimate the optimal change of measure. Furthermore, the convergence of the modified Newton-Raphson algorithm to the optimal quantizer is shown in the framework of [8] to be bounded by the quantization error. However, the tools used to show it does not apply directly to our context and the proof of the convergence of our modified Newton algorithm to an optimal quantizer is an open question.

4.1.2 Computing the weights and the transition probabilities

Once we have access to the quadratic optimal quantizers Γ_k of the marginals \tilde{X}_k , for $k = 0, \dots, n$ (which are estimated using the Newton-Raphson algorithm described previously) we need to compute the associated weights $\mathbb{P}(\tilde{X}_k \in C_j(\Gamma_k))$, $j = 1, \dots, N_k$, for $k = 0, \dots, n$ or the transition probabilities $\mathbb{P}(\tilde{X}_k \in C_j(\Gamma_k) | \tilde{X}_{k-1} \in C_i(\Gamma_{k-1}))$, $i = 1, \dots, N_k$, $j = 1, \dots, N_{k+1}$. We show in the next result how to compute them.

Proposition 4.1. *Let Γ_{k+1} be a quadratic optimal quantizer for the marginal random variable \tilde{X}_{k+1} . Suppose that the quadratic optimal quantizer Γ_k for \tilde{X}_k and its companion weights $\mathbb{P}(\tilde{X}_k \in C_i(\Gamma_k))$, $i = 1, \dots, N_k$, are computed.*

1. *The transition probability $\mathbb{P}(\tilde{X}_{k+1} \in C_j(\Gamma_{k+1}) | \tilde{X}_k \in C_i(\Gamma_k))$ is given by*

$$\mathbb{P}(\tilde{X}_{k+1} \in C_j(\Gamma_{k+1}) | \tilde{X}_k \in C_i(\Gamma_k)) = \left(\Phi'_0(x_{k+1,j+}(x_i^k)) - \Phi'_0(x_{k+1,j-}(x_i^k)) \right) \mathbb{P}(\tilde{X}_k \in C_i(\Gamma_k)). \quad (32)$$

2. *The probability $\mathbb{P}(\tilde{X}_{k+1} \in C_j(\Gamma_{k+1}))$ is given for every $j = 1, \dots, N_{k+1}$ by*

$$\mathbb{P}(\tilde{X}_{k+1} \in C_j(\Gamma_{k+1})) = \sum_{i=1}^{N_k} \left(\Phi'_0(x_{k+1,j+}(x_i^k)) - \Phi'_0(x_{k+1,j-}(x_i^k)) \right) \mathbb{P}(\tilde{X}_k \in C_i(\Gamma_k)). \quad (33)$$

Proof. 1. For every $k \in \{1, \dots, n-1\}$, for every $i = 1, \dots, N_k$ and for every $j = 1, \dots, N_{k+1}$, we have

$$\begin{aligned} \mathbb{P}(\tilde{X}_{k+1} \in C_j(\Gamma_{k+1}) | \tilde{X}_k \in C_i(\Gamma_k)) &= \mathbb{P}(\tilde{X}_{k+1} \in C_j(\Gamma_{k+1}) | \hat{X}_k = x_i^{N_k}) \\ &= \mathbb{P}(\tilde{X}_{k+1} \leq x_{j+1/2}^{N_{k+1}} | \hat{X}_k = x_i^{N_k}) \\ &\quad - \mathbb{P}(\tilde{X}_{k+1} \leq x_{j-1/2}^{N_{k+1}} | \hat{X}_k = x_i^{N_k}) \\ &= \Phi'_0(x_{k+1,j+}(x_i^k)) - \Phi'_0(x_{k+1,j-}(x_i^k)). \end{aligned}$$

2. We have for every $k \in \{1, \dots, n-1\}$ and for every $j = 1, \dots, N_{k+1}$,

$$\begin{aligned} \mathbb{P}(\tilde{X}_{k+1} \in C_j(\Gamma_{k+1})) &= \mathbb{E}[\mathbb{P}(\tilde{X}_{k+1} \in C_j(\Gamma_{k+1}) | \hat{X}_k)] \\ &= \sum_{i=1}^{N_k} \mathbb{P}(\tilde{X}_{k+1} \in C_j(\Gamma_{k+1}) | \hat{X}_k = x_i^{N_k}) \mathbb{P}(\tilde{X}_k \in C_i(\Gamma_k)). \end{aligned}$$

Now, it follows from the first assertion that

$$\mathbb{P}(\tilde{X}_{k+1} \in C_j(\Gamma_{k+1}) | \hat{X}_k = x_i^{N_k}) = \Phi'_0(x_{k+1,j+}(x_i^k)) - \Phi'_0(x_{k+1,j-}(x_i^k)).$$

This completes the proof. \square

5 Numerical examples

5.1 Numerical example for Brownian motion

We consider a real valued Brownian motion $(W_t)_{t \in [0,1]}$ and quantize the random variable W_1 by both regular marginal quantization and recursive marginal quantization methods. Denote by $D_M(\Gamma)$ the regular quantization distortion associated to W_1 and $\tilde{D}_k(\Gamma_k)$, $k = 0, \dots, n$, the sequence of distortions associated to the W_{t_k} 's, $k = 0, \dots, n$, where n is the mesh size and $\Gamma_k = \{w_1^k, \dots, w_{N_k}^k\}$ is a grid of size N_k .

We recall that for a given grid size M , the optimal grid for the regular marginal quantization is obtained by solving (using Newton-Raphson algorithm) the following minimization problem:

$$\inf_{\Gamma \in \mathbb{R}^M} D_M(\Gamma) = \mathbb{E}|W_1 - \widehat{W}_1^\Gamma|^2,$$

which corresponds to the optimal grid of the standard Gaussian distribution. On the other hand, the sequence of recursive marginal quantization grids $(\Gamma_k)_{k=0, \dots, n}$ are defined for every $k = 0, \dots, n$ by

$$\Gamma_k \in \operatorname{argmin}\{\tilde{D}_k(\Gamma), \Gamma \subset \mathbb{R}, \operatorname{card}(\Gamma) \leq N_k\},$$

where

$$\begin{aligned} \tilde{D}_k(\Gamma) &:= \mathbb{E}[d(\tilde{W}_{t_k}, \Gamma)^2] = \mathbb{E}[d(\widehat{W}_{t_{k-1}}^{\Gamma_{k-1}} + \sqrt{\Delta}Z_k, \Gamma)^2] \\ &= \sum_{i=1}^{N_{k-1}} \mathbb{E}[d(w_i^{k-1} + \sqrt{\Delta}Z_k, \Gamma)^2] \mathbb{P}(\widehat{W}_{t_{k-1}}^{\Gamma_{k-1}} = w_i^{k-1}) \end{aligned}$$

and $\widehat{W}_{t_{k-1}}^{\Gamma_{k-1}}$ is defined from the following recursion: $\widehat{W}_0^{\Gamma_0} = 0$ and for $\ell = 1, \dots, k-1$,

$$\widehat{W}_{t_\ell} = \widehat{W}_{t_{\ell-1}}^{\Gamma_{\ell-1}} + \sqrt{\Delta}Z_\ell \text{ and } \widehat{W}_{t_\ell}^{\Gamma_\ell} = \operatorname{Proj}_{\Gamma_\ell}(\widehat{W}_{t_\ell}), (Z_\ell)_{\ell=1, \dots, k} \text{ is i.i.d., and } \mathcal{N}(0; 1)\text{-distributed.}$$

We make a comparison of the quantization errors (the square root of the distortions) obtained from both methods. The result is depicted in Figure 1. In these graphics we fix the mesh size $n = 50$ and we make the total budget $N = N_1 + \dots + N_n$ (given that $N_0 = 1$) of the grid sizes vary 50 by 50, from 250 up to 5000. We choose the sizes N_k following two procedures: without (and with) optimal dispatching, and for both procedures we compare the associated quantization errors with the regular marginal quantization error. In concrete terms, here is how we choose the grid sizes N_k .

▷ WITHOUT OPTIMAL DISPATCHING. For a given global budget N , we make an “equal grid size dispatching” by choosing $N_k = N/n$, for $k = 1, \dots, n$. If for example $N = N_1 + \dots + N_n = 250$, we will have $N_k = 5$, for every $k \in \{1, \dots, n\}$. On the right hand side graphic of Figure 1, we depict the marginal quantization errors $(\tilde{D}_n(\Gamma_n))^{1/2}$, for $|\Gamma_n| = 5, \dots, 100$, and the regular quantization errors $(D_M(\Gamma))^{1/2}$, for $M = |\Gamma| = 5, \dots, 100$.

▷ WITH OPTIMAL DISPATCHING. In this case, the sizes N_k are obtained from the optimal dispatching procedure described in Remark 3.2. First of all, we have to choose the coefficients a_ℓ (appearing in Theorem 3.1) corresponding to the Brownian motion. Following, step by step, the proof of Theorem 3.1 and setting $\eta = 1$ (keep in mind that in the Brownian case $x_0 = 0$), we may choose for $\ell = 0, \dots, n = 50$,

$$a_\ell = \left[\sqrt{\frac{2}{\pi}} (4 + \sqrt{\Delta}) (e^{2t_\ell} - 1) \right]^{1/3}.$$

Making N vary from 250 to 5000, the optimal dispatching leads to the following sizes for the grid Γ_n :

$$|\Gamma_n| \in \mathcal{G} = \{6, 8, 9, 10, 11, 13, \dots, 123, 124, 126, 127\}.$$

This means for example that, if $N = 250$, then the grids Γ_k , for $k = 1, \dots, n = 50$, are not of equal size and $|\Gamma_n| = N_n = 6$; if $N = 300$ then $N_n = 8$; \dots ; and if $N = 5000$ then $N_n = 127$.

The graphic on the left hand side of Figure 1 depicts the marginal quantization errors $(\tilde{D}_n(\Gamma_n))^{1/2}$, where $|\Gamma_n|$ is given by the optimal dispatching procedure, and the regular quantization errors $(D_M(\Gamma))^{1/2}$ for $M = |\Gamma_n| \in \mathcal{G}$.

CONCLUSION. The graphics of figure 1 and 2 lead to two observations. The first one is that both recursive marginal quantization (without and with optimal dispatching) of W_1 are more efficient than its regular marginal quantization, especially when the regular quantization grid is of small size. In fact, in the general setting, the search for the optimal grids associated to the marginals of a stochastic process is based on the computation of the gradient (and the Hessian) of the associated distortion function, which are some expectation with respect to these marginal random variables. Since the recursive marginal quantization procedure is based on successive conditionings which are known to reduce the variance, it is not surprising to observe that the recursive marginal quantization method is more successful than the regular marginal quantization method.

The second conclusion is that the recursive marginal quantization method with the optimal dispatching of the grid size over discretization time steps outperform a setting where the grids are of equal sizes, especially, when the global budget $N = N_1 + \dots + N_n$ is small. However, when N increases, the recursive marginal quantization with optimal dispatching becomes more time consuming and at the same time, both methods lead to almost the same results.

In fact, the following heuristic suggests that, in the general setting, the complexity of the recursive marginal quantization method with optimal dispatching is greater than the one with equal size allocation.

PRACTITIONER’S CORNER. Notice that the complexity of the quantization tree $(\Gamma_k)_{k=0, \dots, n}$ for the recursive marginal quantization is of order $\sum_{k=0}^{n-1} N_k N_{k+1}$. Now, assuming that $N_0 = 1$ and that

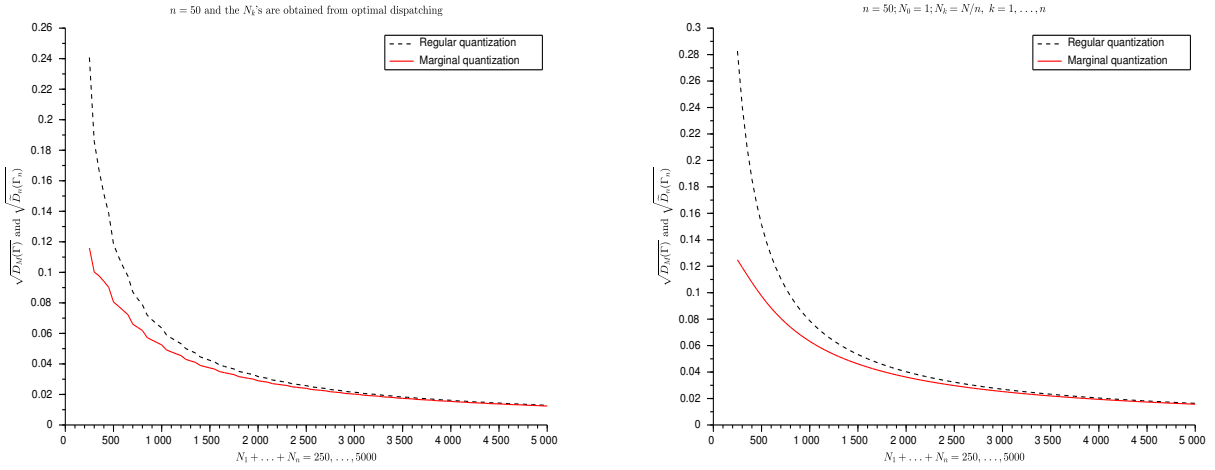


Figure 1: Comparison of the regular marginal quantization (RQ) of W_1 with its recursive marginal quantization (MQ) (where W is a Brownian motion). Abscissa axis: $n = 50$ and the total budget $N = N_1 + \dots + N_n$ varies from 250 up to 5000. Ordinate axis: For a given N , (a) (right hand side graphics) we set $N_k = N/n$, for $k = 1, \dots, n$ and depict the MQ errors $(\tilde{D}_n(\Gamma_n))^{1/2}$, for $|\Gamma_n| = 5, \dots, 100$, and the RQ errors $(D_M(\Gamma))^{1/2}$, for $M = |\Gamma| = 5, \dots, 100$; (b) (left hand side graphic) we depict the MQ errors $(\tilde{D}_n(\Gamma_n))^{1/2}$ where $|\Gamma_n|$ is given by the optimal dispatching procedure, and the RQ errors $(D_M(\Gamma))^{1/2}$ for $M = |\Gamma_n|$.

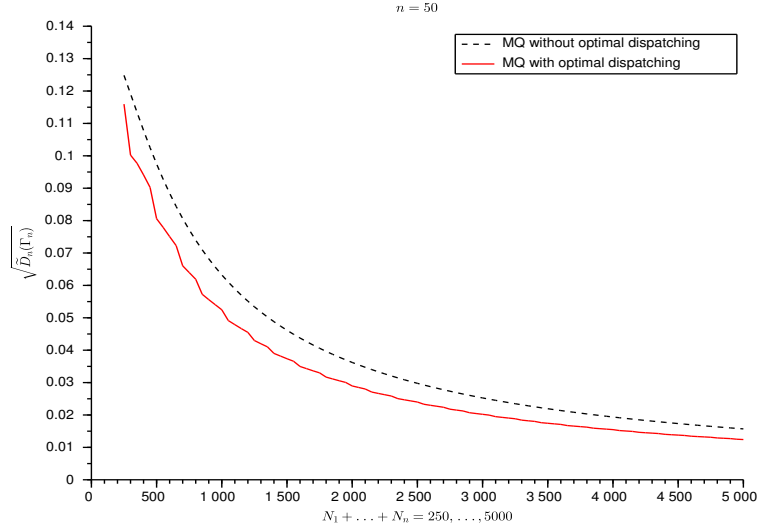


Figure 2: Comparison of the recursive marginal quantization errors. Abscissa axis: $n = 50$ and the total grid sizes $N = N_1 + \dots + N_n$ varies from 250 up to 5000. Ordinate axis: on one hand, we set $N_k = N/n$, for $k = 1, \dots, n$ and depict the recursive marginal quantization errors $(\tilde{D}_n(\Gamma_n))^{1/2}$, for $|\Gamma_n| = 5, \dots, 100$ (MQ without optimal dispatching), and, on the other hand, we depict the marginal quantization errors $(\tilde{D}_n(\Gamma_n))^{1/2}$ where $|\Gamma_n|$ is given by the optimal dispatching procedure (MQ with optimal dispatching).

for every $k = 0, \dots, n-1$, $N_k \leq N_{k+1}$ we want to solve (heuristically) the problem

$$\min \left\{ \sum_{k=0}^{n-1} N_k N_{k+1} \quad \text{subject to} \quad \sum_{k=1}^n N_k = N \right\}. \quad (34)$$

Since $\sum_{k=0}^{n-1} N_k^2 \leq \sum_{k=0}^{n-1} N_k N_{k+1} \leq \sum_{k=1}^n N_k^2$ and that $N_0 = 1$, this suggests that $\sum_{k=0}^{n-1} N_k N_{k+1} \approx \sum_{k=1}^n N_k^2$. Then, if we switch to

$$\min \left\{ \sum_{k=1}^n N_k^2 / N^2 \quad \text{subject to} \quad \sum_{k=1}^n N_k = N \right\} = \min \left\{ \sum_{k=1}^n q_k^2 \quad \text{subject to} \quad \sum_{k=1}^n q_k = 1 \right\}, \quad (35)$$

where $q_k = N_k/N$, it is well known that the solution of the previous problem is given by $q_k = 1/n$, *i.e.*, $N_k = N/n$, for every $k = 1, \dots, n$. Plugging the solution of (35) in (34), this leads to the sub-optimal complexity N^2/n . In fact, any other choice leads to the global complexity

$$\sum_{k=0}^{n-1} q_k q_{k+1} N^2 \geq N^2 \sum_{k=0}^{n-1} q_k^2 \geq N^2 \min \left\{ \sum_{k=0}^n q_k^2 \geq \quad \text{subject to} \quad \sum_{k=0}^n q_k = 1 \right\} > \frac{N^2}{n}.$$

In the next section we propose an application of our method to the pricing of European options in a local volatility models. We remark that when using the marginal quantization methods, we have to choose a big global budget N to reach good price estimates. As in the Brownian case, numerical results show that both recursive marginal quantization methods (with and without optimal dispatching) lead to the same price estimates (up to 10^{-3}) whereas the complexity of the optimal dispatching method becomes higher (as pointed out in the practitioner's corner). This is why we will use in the following section the recursive marginal quantization method without optimal dispatching procedure.

5.2 Pricing of European options in a local volatility model

5.2.1 The model

We consider a pseudo-CEV model (see e.g. [11]) where the dynamics of the stock price process is ruled by the following SDE (under the risk neutral probability)

$$dX_t = rX_t dt + \vartheta \frac{X_t^{\delta+1}}{\sqrt{1+X_t^2}} dW_t, \quad X_0 = x_0, \quad (36)$$

for some $\delta \in (0, 1)$ and $\vartheta \in (0, \vartheta]$ with $\vartheta > 0$. The parameter r stands for the interest rate and $\sigma(x) := \vartheta \frac{x^\delta}{\sqrt{1+x^2}}$ corresponds to the local volatility function. This model becomes very close to the CEV model, specially when the initial value of the stock process X_0 is large enough. In this case the local volatility $\sigma(x) \approx \vartheta x^{\delta-1}$.

We aim at computing the price of a European Put option with payoff $(K - X_T)^+ = \max(K - X_T, 0)$, where K corresponds to the strike of the option and T to its maturity. Then we have to approximate the quantity

$$e^{-rT} \mathbb{E}(K - X_T)^+$$

where \mathbb{E} stands for the expectation under the risk neutral probability. If the process $(\bar{X}_{t_k})_k$ denotes the discrete Euler process at regular time discretization steps t_k , with $0 = t_0 < \dots < t_n = T$, associated to the diffusion process $(X_t)_{t \geq 0}$, this turns out to estimate

$$e^{-rT} \mathbb{E}(K - \bar{X}_T)^+$$

	ϑ	MC (10^5)	MC (10^6)	RMQ
	0.5	0.0022	0.0018	0.0017
CI		[0.0017; 0.0028]	[0.0017; 0.0019]	
	0.6	0.0113	0.0111	0.0110
CI		[0.0101; 0.0125]	[0.0107; 0.0115]	
	0.7	0.0377	0.0373	0.0370
CI		[0.0353; 0.0401]	[0.0366; 0.0381]	
	0.8	0.0883	0.0876	0.0871
CI		[0.0843; 0.0923]	[0.0863; 0.0886]	
	0.9	0.1696	0.1659	0.1649
CI		[0.1635; 0.1756]	[0.1640; 0.1678]	
	1.0	0.267	0.271	0.271
CI		[0.259; 0.275]	[0.269; 0.274]	
	2.0	2.423	2.433	2.426
CI		[2.387; 2.459]	[2.422; 2.445]	
	3.0	5.424	5.492	5.478
CI		[5.424; 5.512]	[5.471; 5.512]	
	4.0	8.893	8.806	8.808
CI		[8.801; 8.986]	[8.777; 8.835]	

Table 1: (Pseudo-CEV model) Comparison of the Put prices obtained from Monte Carlo (MC) simulations (followed by its size) with associated confidence intervals (CI) and from the recursive marginal quantization (RMQ) method. The parameters are: $r = 0.15$; $\delta = 0.5$; $n = 120$; $N_k = 400, \forall k = 1, \dots, n$; $T = 1$; $K = 100$; $X_0 = 100$; and for varying values of ϑ .

	K	MC (10^5)	MC (10^6)	MC (10^7)	RMQ
	100	08.89	08.81	08.81	08.81
CI		[08.80; 08.99]	[08.78; 08.84]	[08.80; 08.82]	
	105	10.61	10.60	10.59	10.59
CI		[10.51; 10.72]	[10.57; 10.63]	[10.58; 10.60]	
	110	12.53	12.57	12.57	12.57
CI		[12.42; 12.64]	[12.53; 12.60]	[12.56; 12.58]	
	115	14.72	14.74	14.75	14.75
CI		[14.60; 14.84]	[14.70; 14.78]	[14.75; 14.77]	
	120	17.18	17.10	17.13	17.12
CI		[17.04; 17.31]	[17.06; 17.15]	[17.11; 17.14]	
	125	19.64	19.69	19.67	19.67
CI		[19.50; 19.78]	[19.64; 19.73]	[19.65; 19.68]	
	130	22.41	22.32	22.40	22.40
CI		[22.26; 22.56]	[22.32; 22.41]	[22.38; 22.41]	

Table 2: (Pseudo-CEV model) Comparison of the Put prices obtained from Monte Carlo (MC) simulations (followed by its size) with associated confidence intervals (CI) and from the recursive marginal quantization (RMQ) method. The parameters are: $r = 0.15$; $n = 120$; $N_k = 400, \forall k = 1, \dots, n$; $T = 1$; $\vartheta = 4$; $X_0 = 100$; and for varying values of K .

by optimal quantization. We estimate this quantity by the recursive marginal quantization method introduced in this paper and compare the numerical results with those obtained from standard Monte Carlo simulations.

5.2.2 Numerical results

To deal with numerical examples we set $\delta = 0.5$, $X_0 = 100$, and choose the interest rate $r = 0.15$. We discretize the price process using the Euler scheme with $n = 120$ (regular) discretization steps and quantize the Euler marginal processes by our proposed method. We put all the marginal quantization grid sizes N_k equals to 400 except for $\hat{X}_0 = X_0 = 100$ which grid size is $N_0 = 1$. We estimate the price of the Put option by

$$\mathbb{E}[(K - \hat{X}_{t_n}^{\Gamma_n})^+] = \sum_{i=1}^{N_n} (K - x_i^{N_n})^+ \mathbb{P}(\hat{X}_{t_n}^{\Gamma_n} = x_i^{N_n}) \quad (37)$$

where $t_n = T$, and where $\Gamma_n = \{x_1^{N_n}, \dots, x_{N_n}^{N_n}\}$ is the quantizer of size N_n computed from the Newton-Raphson algorithm (with 5 iterations) and where the associated weight are estimated from (33).

We compare the prices obtained from the recursive marginal quantization (RMQ) method with those obtained by the Monte Carlo (MC) simulations even for various values of ϑ with a fixed strike $K = 100$ (see Table 1) or for varying values of the strike K with a fixed $\vartheta = 4$ (see Table 2). For the Monte Carlo simulations we set the sample size M_{mc} equal to 10^5 and 10^6 for $K = 100$ and to $M_{\text{mc}} = 10^5, 10^6$ and 10^7 when making the strike K varying.

Remark 5.1. (on the computation time) (a) Remark that all the quantization grids Γ_k of sizes $N_k = 400$, for every $k = 1, \dots, n = 120$, and there companion weights are obtained in around 1 minute from the Newton-Raphson algorithm with 5 iterations. Computations are performed using *Scilab* software on a CPU 2.7 GHz and 4 Go memory computer.

(b) It is clear that once the grids and the associated weights are available, the estimation of the price by RMQ method using the sum (37) is instantaneous (compared to a Monte Carlo simulation).

Remark 5.2. (Initialization of the Newton-Raphson algorithm) Let $0 = t_0 < \dots < t_n$ be the time discretization steps, let $X_0 = x$ be the present value of the stock price process and suppose that the grid sizes N_k are all equal. Since the random variable $\bar{X}_{t_1} \sim \mathcal{N}(m_0(x); v_0^2(x))$, in order to compute the (optimal) N_1 -quantizer for \bar{X}_{t_1} we initialize the algorithm to $v_0(x)z^{N_1} + m_0(x)$, where z^{N_1} is the optimal N_1 -quantizer of the $\mathcal{N}(0; 1)$. Once we get the optimal N_1 -quantization Γ_1 for \bar{X}_{t_1} and its companion weights, we initialize the algorithm to Γ_1 to perform the optimal N_2 -quantizer for \bar{X}_{t_2} and its companion weights, \dots , and so on, until we get the optimal N_n -quantizer for \bar{X}_{t_n} and the associated weights. Notice that doing so we observe no failure of the convergence in all the considered examples.

Remark 5.3. We show in Figure 3 and Figure 4 two graphics where we depict on the abscissa axis the optimal grids (of sizes $N_k = 150$) and on the ordinate axis the corresponding weights. The dynamics of the price process in Figure 3 is given by

$$dX_t = rX_t dt + \sigma X_t dW_t, \quad X_0 = 86.3$$

with $r = 0.03$, $\sigma = 0.05$ whereas its dynamics in Figure 4 is given by

$$dX_t = rX_t dt + \vartheta \frac{X_t^{\delta+1}}{\sqrt{1 + X_t^2}} dW_t, \quad X_0 = 100$$

with $r = 0.15$, $\vartheta = 0.7$, $\delta = 0.5$.

For our numerical examples, we remark first that in all examples the prices obtained by RMQ stay in the confidence interval induced by the MC price estimates. On the other hand the prices obtained by the RMQ method are more precise (more especially when $\vartheta = 4$ and K grows away from 100) than those obtained by the MC method when $M_{\text{mc}} = 10^5$ or 10^6 . Consequently, the RMQ method seems to be more efficient than the MC when the sample size is less than 10^6 . However, when increasing the sample size to $M_{\text{mc}} = 10^7$ the two prices become closer (up to 10^{-2}).

Remark 5.4. We remark that when the Monte Carlo sample size $M_{\text{mc}} = 10^7$ it takes about 2 minutes and 30 seconds to get a price using the *C programming language* on the same computer described previously. Then, in this situation, it takes much more time to obtain a price by MC method than by RMQ.

To strengthen the previous conclusions related to the local volatility model we compare the two methods in the Black-Scholes framework where the stock price process evolves following the dynamics:

$$dX_t = rX_t dt + \sigma X_t dW_t, \quad X_0 = 100.$$

In this setting the true prices are available and will serve us as a support for comparisons. The parameters are chosen so that the model remains close to the Pseudo-CEV model: $r = 0.15$ and $\sigma \approx \vartheta X_0^{\delta-1}$. Numerical results are printed in Tables 3 and Table 4 and confirm our conclusions on the Pseudo-CEV model. We notice that in the Black-Scholes model, the estimated prices from the RMQ method are close to the true prices (the best absolute error is of order 10^{-5} for a volatility $\sigma = 5\%$ and the worse absolute error 2.10^{-2} is achieved with high volatility: $\sigma = 40\%$). This shows the robustness of the RMQ method even for reasonably high values of the volatility.

	σ	MC (10^5)	MC (10^6)	RMQ	True price	Abs. error
	0.05	0.0015	0.00178	0.00176	0.00177	1.10^{-5}
CI		[0.0012; 0.0019]	[0.0017; 0.0019]			
	0.06	0.0116	0.0109	0.0109	0.0112	3.10^{-4}
CI		[0.0104; 0.0128]	[0.0106; 0.0113]			
	0.07	0.0365	0.0370	0.0369	0.0373	4.10^{-4}
CI		[0.0342; 0.0387]	[0.0363; 0.0378]			
	0.08	0.0876	0.0876	0.0869	0.0875	6.10^{-4}
CI		[0.0836; 0.0915]	[0.0863; 0.0888]			
	0.09	0.1666	0.1644	0.1647	0.1654	7.10^{-4}
CI		[0.1607; 0.1724]	[0.1622; 0.1658]			
	0.10	0.269	0.271	0.271	0.272	1.10^{-3}
CI		[0.261; 0.277]	[0.271; 0.273]			
	0.20	2.444	2.431	2.424	2.427	3.10^{-3}
CI		[2.410; 2.479]	[2.420; 2.442]			
	0.30	5.455	5.469	5.470	5.474	4.10^{-3}
CI		[5.395; 5.515]	[5.450; 5.549]			
	0.40	8.680	8.787	8.790	8.792	2.10^{-3}
CI		[8.598; 8.763]	[8.760; 8.813]			

Table 3: (Black-Scholes model) Comparison of the Put prices obtained from Monte Carlo (MC) simulations (followed by its size) with associated confidence intervals (CI) and from the marginal quantization (RMQ) method with the associated absolute error (Abs. error) w. r. t. the true price. The parameters are: $r = 0.15$; $n = 120$; $N_k = 400$, $\forall k = 1, \dots, n$; $T = 1$; $K = 100$; $X_0 = 100$ for varying values of σ .

	K	MC (10^5)	MC (10^6)	RMQ	True price	Abs. error
CI	100	8.680 [8.598; 8.763]	8.787 [8.760; 8.813]	8.790	8.792	2.10^{-3}
	105	10.805 [10.71; 10.90]	10.739 [10.71; 10.90]	10.744	10.750	6.10^{-3}
CI	110	12.86 [12.76; 12.96]	12.89 [12.86; 12.93]	12.90	12.91	1.10^{-2}
	115	15.29 [15.18; 15.40]	15.24 [15.21; 15.28]	15.26	15.27	1.10^{-2}
CI	120	17.66 [17.54; 17.79]	17.81 [17.78; 17.85]	17.79	17.81	1.10^{-2}
	125	20.56 [20.43; 20.69]	20.50 [20.46; 20.54]	20.50	20.52	1.10^{-2}
CI	130	23.28 [23.14; 23.42]	23.37 [23.34; 23.43]	23.37	23.39	2.10^{-2}

Table 4: (Black-Scholes model) Comparison of the Put prices obtained from Monte Carlo (MC) simulations (followed by the size of the MC between brackets) with associated confidence intervals (CI) and from the marginal quantization (RMQ) method with the associated absolute error (Abs. error) w. r. t. the true price. The parameters are: $r = 0.15$; $n = 120$; $N_k = 400, \forall k = 1, \dots, n$; $T = 1$; $\sigma = 40\%$; $X_0 = 100$ for varying values of K .

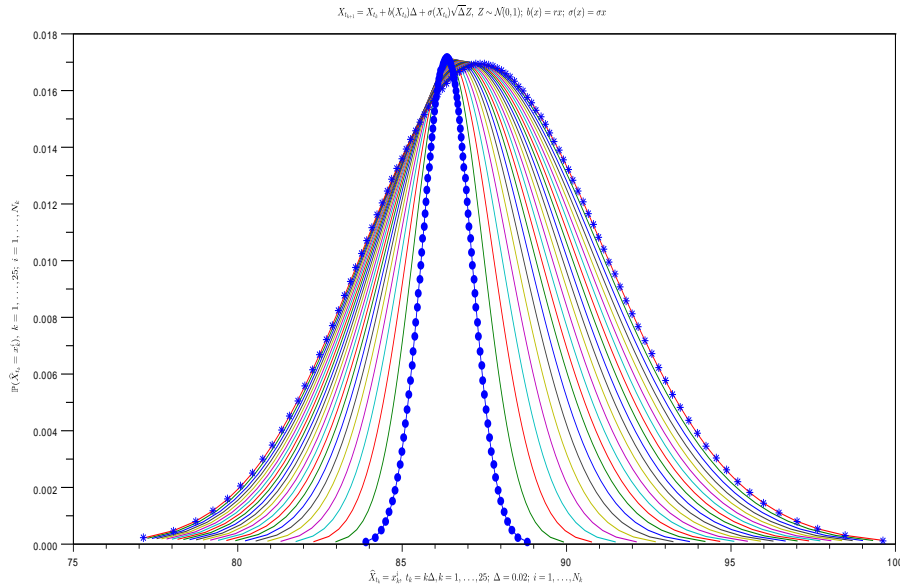


Figure 3: ("Black-Scholes model ") $dX_t = rX_t dt + \sigma X_t dW_t$, $X_0 = 86.3$, $r = 0.03$, $\sigma = 0.05$. Abscissa axis: the optimal grids, $\widehat{X}_{t_k} = x_k^i$, $t_k = k\Delta$, $\Delta = 0.02$, $k = 1, \dots, 25$, $i = 1, \dots, N_k$. Ordinate axis: the associated weights, $\mathbb{P}(\widehat{X}_{t_k} = x_k^i)$, $k = 1, \dots, 25$, $i = 1, \dots, N_k$. \widehat{X}_{t_1} is depicted in dots '•', $\widehat{X}_{t_{25}}$ is represented by the symbol '*'. $t_1 = 0.02$ and $t_{25} = 0.5$ and the remaining in continuous line

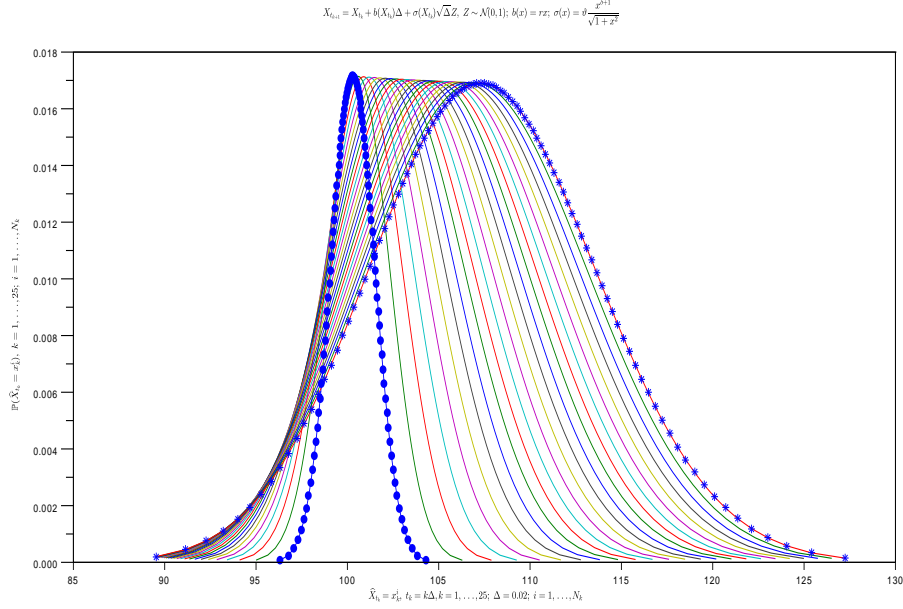


Figure 4: ("Pseudo-CEV model") $dX_t = rX_t dt + \vartheta(X_t^{\delta+1}/(1+X_t^2)^{-1/2})dW_t$, $X_0 = 100$, $r = 0.15$, $\vartheta = 0.7$, $\delta = 0.5$. Abscissa axis: the optimal grids, $\hat{X}_{t_k} = x_k^i$, $t_k = k\Delta$, $\Delta = 0.02$, $k = 1, \dots, 25$, $i = 1, \dots, N_k$. Ordinate axis: the associated weights. \hat{X}_{t_1} is depicted in dots ' \bullet ', $\hat{X}_{t_{25}}$ is represented by the symbol '*', $t_1 = 0.02$ and $t_{25} = 0.5$ and the remaining in continuous line.

Appendix

The proof of Lemma 3.2 needs a additional result we give below as a lemma.

Lemma. Let $a \in \mathbb{R}^d$ et let $p \in (2, 3]$. Then, $\forall u \in \mathbb{R}^d$,

$$|a + u|^p \leq |a|^p + p|a|^{p-2}(a|u) + \frac{p(p+1)}{2}(|a|^{p-2}|u|^2 + |u|^p). \quad (38)$$

Proof. Define the function $g(u) = |u|^p$, $\forall u = (u_1, \dots, u_d) \in \mathbb{R}^d$. We have (denoting by u^* the transpose of the the row vector $u \in \mathbb{R}^d$),

$$\nabla g(u) = p|a + u|^{p-1} \frac{a + u}{|a + u|} \quad \text{and} \quad \nabla^2 g(u) = p(p-2)|a + u|^{p-2} \frac{(a + u)^*(a + u)}{|a + u|^2}.$$

It follows from Taylor-Lagrange formula that

$$|a + u|^p = |a|^p + p|a|^{p-2}(a|u) + \frac{p(p-1)}{2} \frac{|a + \xi|^{p-2}}{|a + u|^2} |u^*((a + u)^*(a + u))u| + p|a + \xi|^{p-2}|u|^2,$$

where $(\cdot|\cdot)$ stands for the inner product and where $\xi = \lambda_u u$, $\lambda_u \in [0, 1]$. However, owing to Cauchy-Schwarz inequality we have

$$|u^*((a + u)^*(a + u))u| \leq |a + u|^2 |u|^2$$

so that

$$\begin{aligned} |a + u|^p &\leq |a|^p + p|a|^{p-2}(a|u) + \frac{p(p-1)}{2}|a + \xi|^{p-2}|u|^2 + p|a + \xi|^{p-2}|u|^2 \\ &\leq |a|^p + p|a|^{p-2}(a|u) + \frac{p(p+1)}{2}|a + \xi|^{p-2}|u|^2. \end{aligned}$$

Then, the result follows since $|a + \xi|^{p-2} \leq |a|^{p-2} + |\xi|^{p-2}$ (because $p-2 \in (0, 1]$) and $|\xi| \leq |u|$. \square

We are now in position to prove Proposition 3.2.

Proof. (of Lemma 3.2.) The proof will be split into three steps.

STEP 1. Let A be a $d \times q$ -matrix. We prove that for any random variable Z such that $\mathbb{E}(Z) = 0$ and $Z \in L^p(\Omega, \mathcal{A}, \mathbb{P})$

$$\mathbb{E}|a + \sqrt{\Delta}AZ|^p \leq \left(1 + \frac{(p+1)(p-2)}{2}\Delta\right)|a|^p + \Delta\left(1 + p + \Delta^{\frac{p}{2}-1}\right)\|A\|^p\mathbb{E}|Z|^p,$$

where $\|A\|^2 = \text{Tr}(AA^*)$. In fact, it follows from Equation (38) that

$$|a + \sqrt{\Delta}AZ|^p \leq |a|^p + p\Delta^{\frac{1}{2}}|a|^{p-2}(a|AZ) + \frac{p(p+1)}{2}(|a|^{p-2}\Delta|AZ|^2 + \Delta^{\frac{p}{2}}|AZ|^p).$$

Applying Young's inequality with conjugate exponents $p' = \frac{p}{p-2}$ and $q' = \frac{p}{2}$, we get

$$|a|^{p-2}\Delta|AZ|^2 \leq \Delta\left(\frac{|a|^p}{p'} + \frac{|AZ|^p}{q'}\right),$$

which leads to

$$\begin{aligned} |a + \sqrt{\Delta}AZ|^p &\leq |a|^p + p\Delta^{\frac{1}{2}}|a|^{p-2}(a|AZ) + \frac{p(p+1)}{2}\left(\frac{\Delta}{p'}|a|^p + \left(\frac{\Delta}{q'} + \Delta^{\frac{p}{2}}\right)|AZ|^p\right) \\ &\leq |a|^p\left(1 + \frac{p(p+1)}{2p'}\Delta\right) + p\Delta^{\frac{1}{2}}|a|^{p-2}(a|AZ) + \Delta\left(\frac{p(p+1)}{2q'} + \Delta^{\frac{p}{2}-1}\right)|AZ|^p. \end{aligned}$$

Taking the expectation yields (owing to the fact that $\mathbb{E}(Z) = 0$)

$$\mathbb{E}|a + \sqrt{\Delta}AZ|^p \leq \left(1 + \frac{(p+1)(p-2)}{2}\Delta\right)|a|^p + \Delta\left(1 + p + \Delta^{\frac{p}{2}-1}\right)\mathbb{E}|AZ|^p.$$

As a consequence, we get

$$\mathbb{E}|a + \sqrt{\Delta}AZ|^p \leq \left(1 + \frac{(p+1)(p-2)}{2}\Delta\right)|a|^p + \Delta\left(1 + p + \Delta^{\frac{p}{2}-1}\right)\|A\|^p\mathbb{E}|Z|^p.$$

STEP 2. Keeping in mind the result of the first step and setting for every $t \in [0, T]$ and $x \in \mathbb{R}^d$, $a := x + \Delta b(t, x)$ and $A := \sigma(t, x)$, we get (owing to the linear growth assumption on the coefficients of the diffusion process)

$$|a| \leq |x|(1 + L\Delta) + L\Delta \quad \text{and} \quad \|A\|^p \leq L_p(1 + |x|^p),$$

where $L_p = 2^{p-1}L^p$. It follows that (keep in mind that $p \in (2, 3]$)

$$\begin{aligned} |a|^p &\leq (1 + 2L\Delta)^p\left(\frac{1 + L\Delta}{1 + 2L\Delta}|x| + \frac{L\Delta}{1 + 2L\Delta}\right)^p \\ &\leq (1 + 2L\Delta)^p\left(\frac{1 + L\Delta}{1 + 2L\Delta}|x|^p + \frac{L\Delta}{1 + 2L\Delta}\right) \\ &\leq (1 + 2L\Delta)^p|x|^p + (1 + 2L\Delta)^{p-1}L\Delta. \end{aligned}$$

Then, we derive

$$\begin{aligned}\mathbb{E}|a + \sqrt{\Delta}AZ|^p &\leq \left(1 + \frac{(p+1)(p-2)}{2}\Delta\right)(1 + 2L\Delta)^p|x|^p \\ &\quad + \left(1 + \frac{(p+1)(p-2)}{2}\Delta\right)(1 + 2L\Delta)^{p-1}L\Delta \\ &\quad + \Delta L_p \left(1 + p + \Delta^{\frac{p}{2}-1}\right)(1 + |x|^p) \mathbb{E}|Z|^p.\end{aligned}$$

Using the inequality $1 + u \leq e^u$, for every $u \in \mathbb{R}$, we finally get

$$\mathbb{E}|a + \sqrt{\Delta}AZ|^p \leq \left(e^{\kappa_p\Delta} + K_p\Delta\right)|x|^p + \left(e^{\kappa_p\Delta}L + K_p\right)\Delta,$$

where $\kappa_p := \left(\frac{(p+1)(p-2)}{2} + 2pL\right)$ and $K_p := L_p \left(1 + p + \Delta^{\frac{p}{2}-1}\right) \mathbb{E}|Z|^p$.

STEP 3. Now, owing to the previous step and to the fact that for every $k = 1, \dots, n$, Z_k is independent from \widehat{X}_{k-1} , we have

$$\begin{aligned}\mathbb{E}|\widetilde{X}_k|^p &= \mathbb{E}\left[\mathbb{E}\left(|\mathcal{E}_k(\widehat{X}_{k-1}, Z_k)|^p \mid \widehat{X}_{k-1}\right)\right] \\ &\leq \left(e^{\kappa_p\Delta} + K_p\Delta\right)\mathbb{E}|\widehat{X}_{k-1}|^p + \left(e^{\kappa_p\Delta}L + K_p\right)\Delta.\end{aligned}$$

Since by construction, \widehat{X}_k is a stationary quantizer (with respect to \widetilde{X}_k) for every $k = 0, \dots, n$, we get

$$\begin{aligned}\mathbb{E}|\widetilde{X}_k|^p &= \left(e^{\kappa_p\Delta} + K_p\Delta\right)\mathbb{E}\left|\mathbb{E}(\widetilde{X}_{k-1} \mid \widehat{X}_{k-1})\right|^p + \left(e^{\kappa_p\Delta}L + K_p\right)\Delta \\ &\leq \left(e^{\kappa_p\Delta} + K_p\Delta\right)\mathbb{E}\left(\mathbb{E}\left(|\widetilde{X}_{k-1}|^p \mid \widehat{X}_{k-1}\right)\right) + \left(e^{\kappa_p\Delta}L + K_p\right)\Delta \quad (\text{Jensen's inequality}) \\ &= \left(e^{\kappa_p\Delta} + K_p\Delta\right)\mathbb{E}|\widetilde{X}_{k-1}|^p + \left(e^{\kappa_p\Delta}L + K_p\right)\Delta.\end{aligned}$$

We show by induction that for every $k = 1, \dots, n$,

$$\begin{aligned}\mathbb{E}|\widetilde{X}_k|^p &\leq \left(e^{\kappa_p\Delta} + K_p\Delta\right)^k \mathbb{E}|\widetilde{X}_0|^p + \left(e^{\kappa_p\Delta}L + K_p\right)\Delta \sum_{j=0}^{k-1} \left(e^{\kappa_p\Delta} + K_p\Delta\right)^j \\ &\leq e^{\kappa_p\Delta k} \left(1 + K_p\Delta e^{-\kappa_p\Delta}\right)^k |x_0|^p + \left(e^{\kappa_p\Delta}L + K_p\right)\Delta \sum_{j=0}^{k-1} e^{\kappa_p\Delta j} \left(1 + K_p\Delta e^{-\kappa_p\Delta}\right)^j.\end{aligned}$$

Using the inequality $1 + u \leq e^u$, for every $u \in \mathbb{R}$, yields

$$\begin{aligned}\mathbb{E}|\widetilde{X}_k|^p &\leq e^{\kappa_p\Delta k} \left(1 + K_p\Delta\right)^k |x_0|^p + \left(e^{\kappa_p\Delta}L + K_p\right)\Delta \sum_{j=0}^{k-1} e^{\kappa_p\Delta j} \left(1 + K_p\Delta\right)^j \\ &\leq e^{(\kappa_p + K_p)\Delta k} |x_0|^p + \left(e^{\kappa_p\Delta}L + K_p\right)\Delta \sum_{j=0}^{k-1} e^{(\kappa_p + K_p)\Delta j} \\ &= e^{(\kappa_p + K_p)t_k} |x_0|^p + \Delta \left(e^{\kappa_p\Delta}L + K_p\right) \frac{e^{(\kappa_p + K_p)t_k} - 1}{e^{(\kappa_p + K_p)\Delta} - 1} \\ &\leq e^{(\kappa_p + K_p)t_k} |x_0|^p + \left(e^{\kappa_p\Delta}L + K_p\right) \frac{e^{(\kappa_p + K_p)t_k} - 1}{\kappa_p + K_p}.\end{aligned}$$

The last inequality follows from the fact that $e^{(\kappa_p + K_p)\Delta} - 1 \geq (\kappa_p + K_p)\Delta$. \square

References

- [1] V. Bally and G. Pagès. A quantization algorithm for solving discrete time multidimensional optimal stopping problems, *Bernoulli*, 9(6), 1003-1049, 2003.
- [2] V. Bally, G. Pagès and J. Printems. A quantization tree method for pricing and hedging multidimensional American options. *Mathematical Finance*, 15(1), 119-168, 2005.
- [3] V. Bally and D. Talay. The law of the Euler scheme for stochastic differential equations (II): convergence rate of the density. *Monte Carlo Methods and Applications*, 2, 93-128, 1996.
- [4] O. Bardou, S. Bouthemy and G. Pagès. Optimal quantization for pricing of swing options. *Applied Mathematical Finance*, 16(2), 183-217, 2009.
- [5] J. A. Bucklew and G. L. Wise. Multidimensional asymptotic quantization theory with r -th power distribution measures. *IEEE Trans. Inform. Theory*, 28, 239-247, 1982.
- [6] G. Callegaro, A. Sagna. An application to credit risk of optimal quantization methods for nonlinear filtering. *The Journal of Computational Finance*, 16, 123-156, 2013.
- [7] M. Corsi, H. Pham and W. Runggaldier. Numerical approximation by quantization of control problems in finance under partial observations. *Mathematical modeling and numerical methods in finance, special volume of Handbook of Numerical analysis*, 2009.
- [8] N. Frikha and A. Sagna. Quantization based recursive Importance Sampling. *Monte Carlo Methods and Applications*, 18, 287-326, 2012.
- [9] A. Gersho and R. Gray. *Vector Quantization and Signal Compression*. Kluwer Academic Press, Boston, 1992.
- [10] S. Graf and H. Luschgy. *Foundations of Quantization for Probability Distributions*. Lect. Notes in Math., 1730, 2000. Berlin: Springer.
- [11] V. Lemaire and G. Pagès. Unconstrained Recursive Importance Sampling. *Annals of Applied Probability*, 20, 1029-1067, 2010.
- [12] H. Luschgy and G. Pagès. Functional quantization and mean regularity of processes with an application to Lévy processes. *The Annals of Applied Probability*, 18(2), 427-469, 2008.
- [13] G. Pagès. A space quantization method for numerical integration. *Journal of Computational and Applied Mathematics*, 89, 1-38, 1998.
- [14] G. Pagès and H. Pham. Optimal quantization methods for nonlinear filtering with discrete time observations. *Bernoulli*, 11(5), 893-932, 2005.
- [15] G. Pagès, H. Pham and J. Printems. An Optimal markovian quantization algorithm for multidimensional stochastic control problems. *Stochastics and Dynamics*, 4(4), 501-545, 2004.
- [16] G. Pagès and J. Printems. Optimal quadratic quantization for numerics: the gaussian case. *Monte Carlo Methods and Applications*, 9(2), 135-165, 2003.
- [17] G. Pagès and J. Printems. Functional quantization for numerics with an application to option pricing. *Monte Carlo Methods and Applications*, 11(4), 407-446, 2005.
- [18] G. Pagès and A. Sagna. Asymptotics of the maximal radius of an L^r -optimal sequence of quantizers. *Bernoulli*, 18(1), 360-389, 2012.

- [19] G. Pagès and J. Yu. Pointwise convergence of the Lloyd algorithm in higher dimension. *Preprint LPMA*.
- [20] H. Pham, W. Runggaldier and A. Sellami. Approximation by quantization of the filter process and applications to optimal stopping problems under partial observation. *Monte Carlo Methods and Applications*, 11, 57-82, 2005.
- [21] C. Profeta and A. Sagna. Conditional hitting time estimation in a nonlinear filtering model by the Brownian bridge method. Preprint. Submitted work.
- [22] A. Sagna. Pricing of barrier options by marginal functional quantization method. *Monte Carlo Methods and Applications*, 17(4), 371-398, 2012.
- [23] W. F. Sheppard. On the Calculation of the Most Probable Values of Frequency-Constants, for Data Arranged According to Equidistant Divisions of Scale, *Proc. London Math. Soc.* 29, 353-380, 1898.
- [24] D. Talay and L. Tubaro. Expansion of the global error for numerical schemes solving stochastic differential equations. *Stochastic Analysis and Applications*, 8(4), 94-120, 1990.
- [25] R. Usmani, Inversion of a tridiagonal Jacobi matrix. *Linear Algebra Appl.*, 212/213, 413-414, 1994.
- [26] P. Zador. Asymptotic quantization error of continuous signals and the quantization dimension. *IEEE Trans. Inform. Theory*, 28, 139-149, 1982.